

Splitting methods for SDEs with locally Lipschitz drift. An illustration on the FitzHugh-Nagumo model

Evelyn Buckwar^{*†}, Adeline Samson[‡], Massimiliano Tamborrino[§], Irene Tubikanec^{*}

Abstract

In this article, we construct and analyse explicit numerical splitting methods for a class of semi-linear stochastic differential equations (SDEs) with additive noise, where the drift is allowed to grow polynomially and satisfies a global one-sided Lipschitz condition. The methods are proved to be mean-square convergent of order 1 and to preserve important structural properties of the SDE. In particular, first, they are hypoelliptic in every iteration step. Second, they are geometrically ergodic and have asymptotically bounded second moments. Third, they preserve oscillatory dynamics, such as amplitudes, frequencies and phases of oscillations, even for large time steps. Our results are illustrated on the stochastic FitzHugh-Nagumo model and compared with known mean-square convergent tamed/truncated variants of the Euler-Maruyama method. The capability of the proposed splitting methods to preserve the aforementioned properties makes them applicable within different statistical inference procedures. In contrast, known Euler-Maruyama type methods commonly fail in preserving such properties, yielding ill-conditioned likelihood-based estimation tools or computationally infeasible simulation-based inference algorithms.

Keywords

Stochastic differential equations, Locally Lipschitz drift, Hypoellipticity, Ergodicity, FitzHugh-Nagumo model, Splitting methods, Mean-square convergence

AMS subject classifications

60H10, 60H35, 65C20, 65C30

Acknowledgements

E.B. was supported by the LCM – K2 Center within the framework of the Austrian COMET-K2 program. A.S. was supported by MIAI@Grenoble Alpes, (ANR-19-P3IA-0003). E.B., M.T. and I.T. were supported by the Austrian Science Fund (FWF): W1214-N15, project DK14. All authors were supported by the Austrian Exchange Service (OeAD), bilateral project FR 03/2017.

1 Introduction

The aim of this article is to construct and analyse splitting methods for semi-linear stochastic differential equations (SDEs) of additive noise type

$$dX(t) = F(X(t))dt + \Sigma dW(t) := (AX(t) + N(X(t)))dt + \Sigma dW(t), \quad X(0) = X_0, \quad t \in [0, T], \quad (1)$$

^{*}Institute for Stochastics, Johannes Kepler University Linz (Evelyn.Buckwar@jku.at, Irene.Tubikanec@jku.at)

[†]Centre for Mathematical Sciences, Lund University

[‡]Laboratoire Jean Kuntzmann, University Grenoble Alpes (Adeline.Leclercq-Samson@univ-grenoble-alpes.fr)

[§]Department of Statistics, University of Warwick (Massimiliano.Tamborrino@warwick.ac.uk)

where the diffusion matrix Σ may be degenerate and the drift F satisfies a global one-sided Lipschitz condition and is allowed to grow polynomially. Coefficients with these properties appear in many applications [25], ranging from physics [40, 46] over population growth problems [28, 32] to neuroscience [18, 23, 49] and others. As an illustrative equation from this class of SDEs, we discuss the stochastic FitzHugh-Nagumo (FHN) model [5, 7, 36], a well-known neuronal model describing the generation of spikes of single neurons at the intracellular level. Our aim is to construct numerical methods for SDE (1), which are easy to implement and also applicable across different disciplines in the broad field of statistical inference. This implies that the developed numerical methods need to meet several requirements:

- Statistical applications require strong approximations of SDEs. Thus, we focus on the concept of *mean-square convergence* of order $p > 0$ [33], i.e., there exists $c > 0$ such that for sufficiently small Δ the inequality

$$\max_{0 \leq t_i \leq T} \left(\mathbb{E} \left[\|X(t_i) - \tilde{X}(t_i)\|^2 \right] \right)^{1/2} \leq c\Delta^p \quad (2)$$

holds, where t_i are time points of a discretised time interval $[0, T]$ with equidistant time steps $\Delta = t_i - t_{i-1}$. In (2), $X(t_i)$ and $\tilde{X}(t_i)$ denote the true and the numerical solution of (1) at the discrete time points t_i , respectively, and $\|\cdot\|$ is the Euclidean norm. Since it was shown in [26] that the standard Euler-Maruyama method does not converge in the mean-square sense under the above assumptions on the drift F , the development of mean-square convergent variants of this method has received much attention. In particular, tamed [27, 56, 62] and truncated [25, 38, 39] Euler-Maruyama methods have been proposed. They all aim to control the unbounded growth arising from the non-globally Lipschitz drift by enforcing a rescaling modification to the drift and/or diffusion coefficients.

- Simulation-based statistical methods require to generate paths of SDEs as computationally efficient as possible, see, e.g., [10]. Using *explicit* numerical methods is a first step to achieve sufficiently low computational cost. While the aforementioned mean-square convergent variants of the Euler-Maruyama method are explicit, they commonly fail in preserving important structural properties of the SDE. The major key to computational efficiency, however, is to construct explicit methods which are capable to preserve the underlying properties of the SDE for time steps as large as possible. This leads to the next point.
- An important issue in the field of (stochastic) numerical analysis is the *preservation of structural properties* of the considered SDE by the numerical methods used to approximate it. Geometric Numerical Integration is a well-established framework in this context [20]. Here, we discuss the preservation of hypoellipticity, geometric ergodicity and oscillatory dynamics such as amplitudes, frequencies and phases of oscillations:
 - The diffusion matrix Σ of SDE (1) may be of full rank or degenerate, where in the latter case the SDE may be *hypoelliptic*. The case of degenerate noise naturally occurs in many applications [2, 17, 35, 36, 40, 46] and the hypoelliptic property ensures that the solution of the SDE admits a smooth transition density [50]. This means that the noise is propagated through the whole system via the drift of the SDE, even though it does not act directly on all components. In many inference approaches using discrete approximations of SDEs, it is necessary that a discrete analogue of the hypoelliptic property holds at each iteration step. In particular, the distribution of $\tilde{X}(t_i)$ given the previous value $\tilde{X}(t_{i-1})$ must admit a smooth density, a property that we term 1-step hypoellipticity. It is known that Euler-Maruyama type methods do not satisfy this. Thus, they yield non-invertible conditional covariance matrices, and, consequently, ill conditioned likelihood-based inference methods [17, 42, 52]. Higher-order Taylor approximation methods [33] may be 1-step hypoelliptic [17]. However, since such methods are also not mean-square convergent in the case of superlinearly growing coefficients [26], and yield

covariance matrices with unpreserved order of magnitude with respect to the time step [17], they lead again to ill-posed statistical problems.

- The analysis of the asymptotic behaviour of the process is of further crucial interest. In particular, if SDE (1) possesses an underlying Lyapunov structure, it may be *geometrically ergodic* [40]. This property ensures that the distribution of the process converges exponentially fast to a unique limit for any starting value X_0 , and has two important statistical implications. First, the choice of the initial value X_0 is negligible since its impact on the distribution of the process decreases exponentially fast. This is particularly relevant, since X_0 is usually not known, especially when the process is only partially observed. Second, there is a correspondence of “time averages along trajectories” and “space averages across trajectories” of geometrically ergodic systems, see, e.g., [2, 16]. This means that quantities related to the distribution of the process can be estimated from a single path simulated over a sufficiently large time horizon instead of relying on repeated simulations of trajectories. For the importance of this feature in statistical inference algorithms, we refer, e.g., to [10]. These two features are only useful when they are preserved by the numerical method used to approximate the geometrically ergodic process. Euler-Maruyama type methods tend to lose the Lyapunov structure of the SDE, not preserving this property [2, 40]. In particular, here, we illustrate that they react sensitively to the starting condition X_0 , and that they may yield poor approximations of the underlying invariant density of the process.
- The last structural properties we are focusing on are features linked to oscillatory dynamics such as *amplitudes*, *frequencies* and *phases* of oscillations. Already in the deterministic scenario it has been observed that Euler type methods may not preserve amplitudes and frequencies of oscillations, see, e.g., [11, 20]. Similar findings have been made for Euler-Maruyama type methods in the stochastic case. For example, it has been proved that the Euler-Maruyama method does not preserve the linear growth rate of linear stochastic harmonic oscillators, overshooting the amplitudes of the underlying oscillations, even for arbitrarily small time steps Δ [61]. Similar non-preserving results of oscillation amplitudes have been observed for non-linear, ergodic and higher-dimensional stochastic oscillators [2, 12, 14]. Taming/truncating perturbations do not improve this behaviour. Even worse, taming perturbations may also lead to a non-preservation of frequencies of oscillations [29, 30]. This lack of amplitude and frequency preservation is confirmed by our numerical experiments on the FHN model. Moreover, we find that Euler-Maruyama type methods may also not preserve phases of oscillations. This poor behaviour is linked to the non-preservation of geometric ergodicity.

Here, we propose to apply *splitting methods* for the approximation of paths of SDE (1), an approach that addresses all previously listed issues. The general idea of this technique is to split the SDE into explicitly solvable subequations, to derive their solutions, and to compose them in a suitable way. We refer to [6, 41] for a thorough discussion of splitting methods for ordinary differential equations (ODEs) and to [1, 2, 8, 9, 12, 35, 44, 47, 51, 57] for articles considering extensions to SDEs. Note that it is often possible to split the differential equation under consideration into different sets of subequations, the choice of the most useful set depending on the problem to be solved. For the class of SDEs with additive noise, where the drift F consists of a linear and a non-linear term, i.e., $F(X(t)) = AX(t) + N(X(t))$, as in Equation (1), the idea is to treat the nonlinear term $N(X(t))$ via a deterministic differential subequation and to solve the remaining linear stochastic subequation explicitly. When N is globally Lipschitz continuous and uniformly bounded, this idea has been applied to the Jansen and Rit neural mass model in [2], and for locally Lipschitz N it has been applied to the Allen-Cahn equation in [9]. Here, we require the ODE with the non-linear term N to be explicitly solvable, as it is the case for the FHN model. If this is not possible, a further splitting step may be necessary or a numerical method for locally Lipschitz ODEs may be applied. Finally, composing the derived explicit solutions via the Lie-Trotter [63] and Strang [59] approach, respectively, yields two *explicit* numerical methods for SDE (1).

We provide two versions of proving the boundedness of the second moment of the proposed splitting methods, each based on an additional assumption on the explicit solution of the underlying ODE with locally Lipschitz term N . This result is the key to establish their *mean-square convergence*. In particular, we prove that they converge with order $p = 1$, in agreement with the convergence rate of comparable known splitting methods in the globally Lipschitz scenario [2, 44], and with standard methods such as the Euler-Maruyama method in the case of additive noise [33]. Moreover, we show that the proposed splitting methods are *1-step hypoelliptic* for any time step Δ , provided that the stochastic subequation of the splitting framework is hypoelliptic. The invertability of the resulting covariance matrix is guaranteed by using the information contained in the drift matrix A . In particular, we show that the transition distribution of the Lie-Trotter method corresponds to a non-degenerate multivariate normal distribution. Having a non-degenerate covariance matrix may then allow likelihood-based inference. Furthermore, we prove that the constructed splitting methods satisfy a discrete Lyapunov condition, and are *geometrically ergodic* for any time step Δ . This result requires the assumption that $\|e^{A\Delta}\| < 1$, where the matrix norm is induced by the Euclidean norm. Moreover, we show that the second moments of the splitting methods are asymptotically bounded by constants which are independent of the time step Δ . This result holds if the logarithmic norm [58, 60] of the matrix A is strictly negative. In the one-dimensional case, some of the involved expressions simplify and we obtain precise *closed-form (asymptotic) bounds of the second moments* of the proposed splitting methods. These bounds are illustrated on a cubic one-dimensional model problem with drift given by $F(X(t)) = -X^3(t)$ [26, 40]. In addition, we illustrate the proposed splitting methods on the stochastic FHN model and show through a variety of numerical experiments that they preserve the qualitative dynamics of neuronal spiking, in particular, *amplitudes, frequencies* and *phases* of the underlying oscillations even for large time discretisation steps Δ .

The article is organised as follows. In Section 2, we introduce necessary mathematical preliminaries and notations, and we discuss equations of interest and relevant properties. In Section 3, we present the proposed splitting methods and recall different tamed and truncated variants of the Euler-Maruyama method. In Section 4, we establish the mean-square convergence of the splitting methods. In Section 5, we prove their 1-step hypoellipticity, establish their geometric ergodicity, derive (asymptotic) second moment bounds and illustrate them on a one-dimensional model problem. In Section 6, we apply the proposed splitting approach to the stochastic FHN model and discuss conditions under which the presented results hold. In Section 7, we provide a variety of numerical experiments, illustrating the theoretical results and comparing the considered numerical methods. Conclusions are reported in Section 8.

2 Model and properties

Throughout, the following notations are used.

Notation 2.1. Let $x, y \in \mathbb{R}^d$ be generic vectors. Then x_l denotes the l -th entry of x , x^\top the transpose of x , $\|x\| = (x_1^2 + \dots + x_d^2)^{1/2}$ the Euclidean norm of x and $(x, y) = x_1 y_1 + \dots + x_d y_d$ the scalar product of x and y . Further, let $A, B \in \mathbb{R}^{d \times d}$ be generic matrices. Then a_{lj} denotes the component in the l -th row and j -th column of A , A^\top the transpose of A , 0_d the d -dimensional zero vector and \mathbb{I}_d the $d \times d$ -dimensional identity matrix. Moreover, we denote by $\|A\| = \sqrt{\lambda_{\max}(A^\top A)}$ the matrix norm which is induced by the Euclidean norm, where $\lambda_{\max}(A)$ is the largest eigenvalue of A , and with $\mu(A) = \lambda_{\max}((A + A^\top)/2)$ the real-valued logarithmic norm which results from the Euclidean norm and its induced matrix norm.

Let $(\Omega, \mathcal{F}, \mathbb{P})$ be a complete probability space with filtration $(\mathcal{F}(t))_{t \in [0, T]}$. Furthermore, let $(W(t))_{t \in [0, T]}$ be a m -dimensional Wiener process defined on that space and adapted to $(\mathcal{F}(t))_{t \in [0, T]}$. We consider the d -dimensional autonomous SDE of additive noise type (1)

$$dX(t) = F(X(t))dt + \Sigma dW(t) := (AX(t) + N(X(t)))dt + \Sigma dW(t), \quad X(0) = X_0, \quad t \in [0, T],$$

where $T > 0$, $A \in \mathbb{R}^{d \times d}$, $\Sigma \in \mathbb{R}^{d \times m}$, $F : \mathbb{R}^d \rightarrow \mathbb{R}^d$ and $N : \mathbb{R}^d \rightarrow \mathbb{R}^d$ are locally Lipschitz continuous. The initial value X_0 is an $\mathcal{F}(0)$ -measurable \mathbb{R}^d -valued random variable which is independent of $(W(t))_{t \in [0, T]}$ and such that $\mathbb{E} [\|X_0\|^2] < \infty$. We suppose that SDE (1) has a unique strong solution, which is regular in the sense of [31], i.e., it is defined on the entire interval $[0, T]$ such that sample paths do not blow up to infinity in finite time. Formally, we require the existence of a stochastic process $(X(t))_{t \in [0, T]}$ which is adapted to $(\mathcal{F}(t))_{t \in [0, T]}$ and has continuous paths satisfying

$$X(t) = X_0 + \int_0^t F(X(s)) ds + \int_0^t \Sigma dW(s),$$

for all $t \in [0, T]$ \mathbb{P} -almost surely. Conditions required to ensure the existence of such a process $(X(t))_{t \in [0, T]}$ are, e.g., discussed in [3, 31, 34, 37]. Here, we follow the setting in [27, 29, 62] and suppose that the drift satisfies a global one-sided Lipschitz condition and is allowed to grow polynomially at infinity. It suffices to place these conditions on N :

Assumption 2.1. (A1) *The function N is globally one-sided Lipschitz continuous, i.e., there exists a constant $c_1 > 0$ such that*

$$(x - y, N(x) - N(y)) \leq c_1 \|x - y\|^2, \quad \forall x, y \in \mathbb{R}^d.$$

(A2) *The function N grows at most polynomially, i.e., there exist constants $c_2 > 0$ and $\chi \geq 1$ such that*

$$\|N(x) - N(y)\|^2 \leq c_2(1 + \|x\|^{2\chi-2} + \|y\|^{2\chi-2})\|x - y\|^2, \quad \forall x, y \in \mathbb{R}^d.$$

Assumption 2.1 ensures the finiteness of the moments of the solution of (1) [22, 29, 31, 62]. In particular, there exists a constant $K(T) > 0$ such that

$$\max_{0 \leq t \leq T} \mathbb{E} [\|X(t)\|^2] \leq K(T) \left(1 + \mathbb{E} [\|X_0\|^2]\right).$$

Moreover, the process $(X(t))_{t \in [0, T]}$ is a Markov process. Denoting $\mathcal{B}(\mathbb{R}^d)$ the Borel sigma-algebra on \mathbb{R}^d , its transition probability is defined as

$$P_t(\mathcal{A}, x) := \mathbb{P}(X(t) \in \mathcal{A} | X(0) = x), \quad (3)$$

where $\mathcal{A} \in \mathcal{B}(\mathbb{R}^d)$. This corresponds to the probability that the process reaches a Borel set $\mathcal{A} \subset \mathbb{R}^d$ at time t , provided that it started in $x \in \mathbb{R}^d$ at time $0 < t$.

2.1 Noise structure: ellipticity and hypoellipticity

Depending on the noise structure, two classes of models are obtained. The first class is called *elliptic* and corresponds to SDEs with a non-degenerate diffusion matrix, i.e., $\Sigma \Sigma^\top$ is of full rank such that $\det(\Sigma \Sigma^\top) \neq 0$. In particular, we consider $d = m$ and a diagonal matrix $\Sigma = \text{diag}[\sigma_1, \dots, \sigma_d]$ with $\sigma_j > 0$ for $j = 1, \dots, d$.

The second class corresponds to SDEs with degenerate diffusion matrix, as it naturally occurs in many application models. Following the notion in [17], we consider $m = d - 1$ and Σ given by

$$\Sigma := \begin{pmatrix} 0_{d-1}^\top \\ \Gamma \end{pmatrix}, \quad (4)$$

where $\Gamma = \text{diag}[\sigma_1, \dots, \sigma_{d-1}] \in \mathbb{R}^{(d-1) \times (d-1)}$ is a diagonal matrix with $\sigma_j > 0$ for $j = 1, \dots, d - 1$. The first component of the solution $(X(t))_{t \in [0, T]}$ is called *smooth*, since it is not directly affected by the noise. The remaining $d - 1$ components are called *rough*, because the noise acts directly on

them. In this scenario, SDE (1) is often *hypoelliptic*. It means that the transition probability (3) admits a smooth density, even though $\Sigma\Sigma^\top$ is not of full rank. This is the case when the SDE satisfies the weak Hörmander condition, based on the concept of Lie-brackets [50]. A sufficient and necessary condition for the process $(X(t))_{t \in [0, T]}$ to be hypoelliptic, is that at least one of its rough coordinates appears in the first component $F_1(X(t))$ of the drift [17]. In particular, the following condition is required

$$\forall x \in \mathbb{R}^d, \quad (\partial_r F_1(x), \sigma^j) \neq 0 \quad \text{for at least one } j = 1, \dots, d-1, \quad (5)$$

where σ^j denotes the j -th column vector of Γ and $\partial_r F_1(x) := (\partial_{x_2} F_1(x), \dots, \partial_{x_d} F_1(x))^\top$ is the vector of partial derivatives of the first entry of the drift with respect to the rough components. This setting can be extended to several smooth coordinates by requiring that at least one of the rough coordinates enters the respective components of the drift.

2.2 Lyapunov structure: geometric ergodicity

Here, a particular interest lies in SDEs of type (1) where the drift $F(X(t))$ satisfies the following dissipativity condition

$$(F(x), x) \leq \alpha - \delta \|x\|^2, \quad \forall x \in \mathbb{R}^d, \quad (6)$$

where $\alpha, \delta > 0$. Condition (6) ensures that the function $L : \mathbb{R}^d \rightarrow [1, \infty)$ defined by $L(x) := 1 + \|x\|^2$ is a Lyapunov function for (1), see [40]. That is $L(x) \rightarrow \infty$ as $\|x\| \rightarrow \infty$, and there exist constants $\rho, \eta > 0$ such that

$$\mathcal{L}\{L(x)\} \leq -\rho L(x) + \eta, \quad (7)$$

where \mathcal{L} is the generator of the SDE given by

$$\mathcal{L}\{g(x)\} = \sum_{l=1}^d F_l(x) \frac{\partial g}{\partial x_l}(x) + \frac{1}{2} \sum_{l,j=1}^d [\Sigma\Sigma^\top]_{lj} \frac{\partial^2 g}{\partial x_l \partial x_j}(x),$$

for sufficiently smooth functions $g : \mathbb{R}^d \rightarrow \mathbb{R}$, with $[\Sigma\Sigma^\top]_{lj}$ denoting the entry in the l -th row and j -th column of the matrix $\Sigma\Sigma^\top$. The existence of a Lyapunov function satisfying (7) is the key to establish the *geometric ergodicity* of the solution of (1). This property means that the distribution of the Markov process $(X(t))_{t \in [0, T]}$ converges exponentially fast to a unique invariant distribution π , satisfying

$$\pi(\mathcal{A}) = \int_{\mathbb{R}^d} P_t(\mathcal{A}, x) \pi(dx), \quad \forall \mathcal{A} \in \mathcal{B}(\mathbb{R}^d), \quad t \in [0, T].$$

In particular, if SDE (1) is elliptic, Condition (6) suffices to establish the geometric ergodicity of $(X(t))_{t \in [0, T]}$. If SDE (1) is not elliptic, the process is geometrically ergodic, if, in addition to fulfilling Condition (6) (and thus (7)), it is hypoelliptic and satisfies the irreducibility condition $P_t(\mathcal{A}, x) > 0$ for all open sets $\mathcal{A} \in \mathcal{B}(\mathbb{R}^d)$ and $x \in \mathbb{R}^d$. The reader is referred to [40] and the references therein for further details.

3 Numerical methods

Consider a discretised time interval $[0, T]$ with equidistant time steps $\Delta = t_i - t_{i-1} \in (0, \Delta_0]$, with $\Delta_0 > 0$, $i = 1, \dots, n$, where $t_0 = 0$ and $t_n = T$. Without loss of generality, we consider $\Delta_0 \in (0, 1)$. We denote by $(\tilde{X}(t_i))_{i=0, \dots, n}$ a numerical solution of SDE (1) approximating the process $(X(t))_{t \in [0, T]}$ at t_i , where $\tilde{X}(t_0) := X_0$. We first present splitting methods for Equation (1) and then recall different Euler-Maruyama type methods proposed for SDEs with superlinearly growing drift coefficients.

3.1 Splitting approach

We start by providing a brief account of the main ideas behind the numerical splitting approach [6, 41]. For the sake of simplicity, consider the following ODE

$$dX(t) = F(X(t))dt, \quad X(0) = X_0 \in \mathbb{R}^d, \quad t \in [0, T]. \quad (8)$$

The goal is to derive a numerical method to approximate its solution. Assume that the function $F(X(t))$ can be expressed as

$$F(X(t)) = \sum_{k=1}^N F^{[k]}(X(t)), \quad N \in \mathbb{N}, \quad (9)$$

where $F^{[k]} : \mathbb{R}^d \rightarrow \mathbb{R}^d$. Usually, there are several ways to decompose this function. The goal is to do it in a way such that the solutions of the resulting subequations

$$dX(t) = F^{[k]}(X(t))dt, \quad k = 1, \dots, N, \quad (10)$$

exist on $[0, T]$ and can be derived explicitly. Having derived the explicit solutions of the subequations, the next task is to compose them properly. Two common ways are the so-called Lie-Trotter [63] and the Strang [59] approach. Let $\varphi_t^{[k]}(X_0)$ denote the exact solutions (flows) of the subequations in (10) at time t and starting from X_0 . Then the Lie-Trotter composition of flows

$$\tilde{X}^{\text{LT}}(t_i) = \left(\varphi_{\Delta}^{[1]} \circ \dots \circ \varphi_{\Delta}^{[N]} \right) (\tilde{X}^{\text{LT}}(t_{i-1}))$$

and the Strang approach

$$\tilde{X}^{\text{S}}(t_i) = \left(\varphi_{\Delta/2}^{[1]} \circ \dots \circ \varphi_{\Delta/2}^{[N-1]} \circ \varphi_{\Delta}^{[N]} \circ \varphi_{\Delta/2}^{[N-1]} \circ \dots \circ \varphi_{\Delta/2}^{[1]} \right) (\tilde{X}^{\text{S}}(t_{i-1}))$$

define splitting solutions of ODE (8). Thus, splitting methods consists of three equally important steps:

- (i) Choosing the functions $F^{[k]}(X(t))$ in (9).
- (ii) Deriving the solutions of the subequations in (10).
- (iii) Composing the derived solutions to construct a numerical solution of (8).

This idea can be directly extended to SDEs, where the subequations in (10) may consist of deterministic and/or stochastic dynamical systems.

3.2 Splitting methods for semi-linear SDEs

In this section, we propose a splitting strategy for SDE (1), where

$$F^{[1]}(X(t)) = AX(t) \quad \text{and} \quad F^{[2]}(X(t)) = N(X(t)). \quad (11)$$

Step (i): Choice of the subequations To make use of the treatable underlying stochastic linear dynamics, we propose to split equations of this type into the following two subequations

$$dX^{[1]}(t) = AX^{[1]}(t)dt + \Sigma dW(t), \quad X^{[1]}(0) = X_0^{[1]}, \quad t \in [0, T], \quad (12)$$

$$dX^{[2]}(t) = N(X^{[2]}(t))dt, \quad X^{[2]}(0) = X_0^{[2]}, \quad t \in [0, T]. \quad (13)$$

This splitting strategy is an extension of the method presented in [2], where the authors consider a globally Lipschitz Hamiltonian type equation with uniformly bounded non-linear terms. Our method considers a more general class of coefficients $N(X(t))$, including functions which are allowed to grow polynomially at infinity according to Assumption 2.1.

Step (ii): Explicit solution of the subequations In the following, we discuss the subequations (12) and (13). The first subequation is a linear SDE. It can be solved explicitly, even when the dimension d is large and independent of whether the equation has an elliptic or hypoelliptic noise structure [4, 37]. In particular, the explicit solution of (12) is given by

$$X^{[1]}(t) = e^{At} X_0^{[1]} + \int_0^t e^{A(t-s)} \Sigma dW(s). \quad (14)$$

The Itô integral in (14) is normally distributed with mean 0_d . Moreover, using Itô's isometry and the fact that the components of the Wiener process are independent, its $d \times d$ -dimensional covariance matrix is given by

$$C(t) = \int_0^t e^{A(t-s)} \Sigma \Sigma^\top (e^{A(t-s)})^\top ds. \quad (15)$$

Hence, paths of (12) can be simulated exactly at the discrete time points t_i . In particular,

$$\varphi_\Delta^{[1]}(X^{[1]}(t_{i-1})) := X^{[1]}(t_i) = e^{A\Delta} X^{[1]}(t_{i-1}) + \xi_{i-1}, \quad i = 1, \dots, n, \quad (16)$$

where the ξ_{i-1} are independent and identically distributed d -dimensional Gaussian vectors with mean 0_d and covariance matrix $C(\Delta)$ given by (15).

Regarding the second subequation, the following assumption is made.

Assumption 3.1. (A3) *The function $N : \mathbb{R}^d \rightarrow \mathbb{R}^d$ in (11) is such that the global solution of ODE (13) can be derived explicitly.*

Granting Assumption (A3), the solution of the second subequation can also be obtained exactly at the discrete time points t_i . In particular,

$$\varphi_\Delta^{[2]}(X^{[2]}(t_{i-1})) := X^{[2]}(t_i) = f(X^{[2]}(t_{i-1}); \Delta), \quad i = 1, \dots, n, \quad (17)$$

where $f : \mathbb{R}^d \rightarrow \mathbb{R}^d$ denotes the explicit solution of (13). Assumption (A3) may be relaxed, e.g., by applying a proper numerical method to approximate the solution of (13) [11, 41]. We refer to [21, 24] for an exhaustive discussion of numerical methods for locally Lipschitz ODEs.

Step (iii): Composition of the explicit solutions To finally obtain numerical solutions of the original SDE (1), the explicit solutions (16) and (17) of the subequations (12) and (13) are composed in every iteration step. In particular, we investigate the following methods

$$\tilde{X}^{\text{LT}}(t_i) = \left(\varphi_\Delta^{[1]} \circ \varphi_\Delta^{[2]} \right) (\tilde{X}^{\text{LT}}(t_{i-1})) = e^{A\Delta} f(\tilde{X}^{\text{LT}}(t_{i-1}); \Delta) + \xi_{i-1}, \quad (18)$$

$$\tilde{X}^{\text{S}}(t_i) = \left(\varphi_{\Delta/2}^{[2]} \circ \varphi_\Delta^{[1]} \circ \varphi_{\Delta/2}^{[2]} \right) (\tilde{X}^{\text{S}}(t_{i-1})) = f \left(e^{A\Delta} f(\tilde{X}^{\text{S}}(t_{i-1}); \Delta/2) + \xi_{i-1}; \Delta/2 \right), \quad (19)$$

which are based on the Lie-Trotter (LT) and Strang (S) approach, respectively.

We emphasise that the constructed splitting schemes (18) and (19) are easy to implement. In particular, the matrix exponential $e^{A\Delta}$ and the covariance matrix $C(\Delta)$ have to be computed only once and the normal random variables ξ_{i-1} , $i = 1, \dots, n$, can be obtained using a Cholesky decomposition of the covariance matrix $C(\Delta)$.

3.3 Euler-Maruyama type methods

Let $\psi_{i-1} \sim \mathcal{N}(0_m, \mathbb{I}_m)$, $i = 1, \dots, n$, be independent and identically distributed m -dimensional standard Gaussian vectors. The Euler-Maruyama method [33, 45] used to approximate solutions of SDEs with globally Lipschitz continuous coefficients yields paths of (1) through the iteration

$$\tilde{X}^{\text{EM}}(t_i) = \tilde{X}^{\text{EM}}(t_{i-1}) + F(\tilde{X}^{\text{EM}}(t_{i-1}))\Delta + \Sigma\sqrt{\Delta}\psi_{i-1}. \quad (20)$$

In [26], it has been shown that the Euler-Maruyama method is not mean-square convergent in the sense of (2) if at least one of the coefficients of the SDE grows superlinearly, as this results in unbounded moments of the iterates. Several explicit variants of this method have been proposed, which aim to control this unbounded growth.

The first variant, designed for polynomially growing and one-sided Lipschitz drift and globally Lipschitz diffusion coefficients, has been introduced in [27]. It is based on a taming perturbation which avoids large values caused by the superlinearly growing drift. The method is defined through the iteration

$$\tilde{X}^{\text{TEM}}(t_i) = \tilde{X}^{\text{TEM}}(t_{i-1}) + \frac{F(\tilde{X}^{\text{TEM}}(t_{i-1}))\Delta}{1 + \left\|F(\tilde{X}^{\text{TEM}}(t_{i-1}))\right\|\Delta} + \Sigma\sqrt{\Delta}\psi_{i-1}, \quad (21)$$

and can be rewritten to coincide with the Euler-Maruyama method (20) up to terms of second order. This fact is used to establish the mean-square convergence of order 1/2 (order 1) for SDEs with multiplicative noise (additive noise), i.e., the same rate achieved by the Euler-Maruyama method in the globally Lipschitz case [33].

Another variant, aiming to tame both the drift and the diffusion term, has been suggested in [62]. The method is defined via

$$\tilde{X}^{\text{DTEM}}(t_i) = \tilde{X}^{\text{DTEM}}(t_{i-1}) + \frac{F(\tilde{X}^{\text{DTEM}}(t_{i-1}))\Delta + \Sigma\sqrt{\Delta}\psi_{i-1}}{1 + \left\|F(\tilde{X}^{\text{DTEM}}(t_{i-1}))\right\|\Delta + \left\|\Sigma\sqrt{\Delta}\psi_{i-1}\right\|}, \quad (22)$$

and is designed for the broader class of equations where also the diffusion coefficient is allowed to grow polynomially at infinity and satisfies a one-sided Lipschitz condition. It has been shown to converge with mean-square order 1/2.

The strong convergence (without order) of a related class of variants, based on space truncation techniques, has been discussed in [25]. In particular, we recall the two methods

$$\tilde{X}^{\text{TrEM}}(t_i) = \tilde{X}^{\text{TrEM}}(t_{i-1}) + \frac{F(\tilde{X}^{\text{TrEM}}(t_{i-1}))\Delta}{\max\left\{1, \left\|F(\tilde{X}^{\text{TrEM}}(t_{i-1}))\right\|\Delta\right\}} + \Sigma\sqrt{\Delta}\psi_{i-1}, \quad (23)$$

$$\tilde{X}^{\text{DTrEM}}(t_i) = \tilde{X}^{\text{DTrEM}}(t_{i-1}) + \frac{F(\tilde{X}^{\text{DTrEM}}(t_{i-1}))\Delta + \Sigma\sqrt{\Delta}\psi_{i-1}}{\max\left\{1, \Delta\left\|F(\tilde{X}^{\text{DTrEM}}(t_{i-1}))\Delta + \Sigma\sqrt{\Delta}\psi_{i-1}\right\|\right\}}, \quad (24)$$

constructed to truncate the drift and the drift and diffusion term, respectively.

In the following, we denote by tamed (TEM), diffusion tamed (DTEM), truncated (TrEM) and diffusion truncated (DTrEM) Euler-Maruyama method, the schemes (21), (22), (23) and (24), respectively.

4 Mean-square convergence

In this section, mean-square convergence of the constructed splitting methods is proved. It has been observed in the globally Lipschitz case that splitting methods have the same convergence order as the Euler-Maruyama method (20), i.e., order 1 in the case of additive noise, see, e.g., [2, 44]. We extend this result to the locally Lipschitz case, proving mean-square convergence of order 1 for the proposed splitting methods.

4.1 Required background

To establish this result, we rely on Theorem 2.1 of [62], which provides an extension of Milstein's fundamental theorem on the mean-square order of convergence [43] (see also Theorem 1.1 in [45]) for globally Lipschitz coefficients to the considered setting specified in Assumption 2.1. To facilitate

the illustration of our results, we recall this statement in Theorem 4.1 below, after defining the required ingredients of mean-square consistency and boundedness.

Let $X_{t_{i-1},x}(t_i)$ denote the true solution at time t_i starting from x at time t_{i-1} , i.e., $X(t_{i-1}) = x$, and $\tilde{X}_{t_{i-1},x}(t_i)$ the one-step approximation used to construct a numerical solution $\tilde{X}(t_i)$. In particular, the one-step approximations of the numerical methods discussed in the previous section are defined by (18)-(24), where $\tilde{X}(t_{i-1})$ is replaced by x .

Definition 4.1. *The one-step approximation $\tilde{X}_{t_{i-1},x}(t_i)$ of a numerical solution $\tilde{X}(t_i)$ of SDE (1) is mean-square consistent of order $p > 0$, if there exists $\Delta_0 > 0$ such that for arbitrary t_i , $i = 1, \dots, n$, $x \in \mathbb{R}^d$, and for all $\Delta \in (0, \Delta_0]$ it has the following orders of accuracy*

$$\begin{aligned} \left\| \mathbb{E} \left[X_{t_{i-1},x}(t_i) - \tilde{X}_{t_{i-1},x}(t_i) \right] \right\| &= \mathcal{O}(\Delta^{p+1}), \\ \left(\mathbb{E} \left[\left\| X_{t_{i-1},x}(t_i) - \tilde{X}_{t_{i-1},x}(t_i) \right\|^2 \right] \right)^{1/2} &= \mathcal{O}(\Delta^{p+\frac{1}{2}}). \end{aligned}$$

Besides mean-square consistency, the boundedness of the second moment of the numerical solution has to be proved. In the globally Lipschitz case, this is guaranteed by the linear growth bounds of the coefficients.

Definition 4.2. *A numerical solution $\tilde{X}(t_i)$ of SDE (1) is mean-square bounded, if there exist $\Delta_0 > 0$ and a constant $\tilde{K}(T, \Delta_0) > 0$ such that for all $\Delta \in (0, \Delta_0]$ it holds that*

$$\max_{0 \leq t_i \leq T} \mathbb{E} \left[\left\| \tilde{X}(t_i) \right\|^2 \right] \leq \tilde{K}(T, \Delta_0) \left(1 + \mathbb{E} \left[\|X_0\|^2 \right] \right).$$

Based on the above defined ingredients, the following theorem guarantees mean-square convergence.

Theorem 4.1 (Theorem 2.1 in Tretyakov and Zhang (2013)). *Let $\tilde{X}(t_i)$ denote a numerical solution of SDE (1) at time t_i starting at X_0 , constructed using the one-step approximation $\tilde{X}_{t_{i-1},x}(t_i)$. Further, let Assumptions (A1) and (A2) be satisfied. If*

- (i) *The one-step approximation $\tilde{X}_{t_{i-1},x}(t_i)$ is mean-square consistent of order $p > 0$ in the sense of Definition 4.1.*
- (ii) *The numerical method $\tilde{X}(t_i)$ is mean-square bounded in the sense of Definition 4.2.*

Then the numerical method $\tilde{X}(t_i)$ is mean-square convergent of order p in the sense of (2).

4.2 Mean-square convergence of the splitting methods

In the following, we prove the required Conditions (i) and (ii) of Theorem 4.1 for the constructed splitting methods.

Condition (i) can be proved in a similar fashion as Lemma 2.1 in [44]. Its proof relies on the fact that the Euler-Maruyama method (20) is mean-square consistent of order 1, which is also true in the locally Lipschitz case. Since the tamed Euler-Maruyama method (21) can be written as a sum of the Euler-Maruyama method and a deterministic remainder of second order [27], the same result would be obtained when using this method instead.

Lemma 4.1 (Mean-square consistency). *Let Assumption (A3) hold and let $\tilde{X}_{t_{i-1},x}^{LT}(t_i)$ and $\tilde{X}_{t_{i-1},x}^S(t_i)$ be the one-step approximations of the Lie-Trotter and Strang splitting defined through (18) and (19), respectively. Then $\tilde{X}_{t_{i-1},x}^{LT}(t_i)$ and $\tilde{X}_{t_{i-1},x}^S(t_i)$ are mean-square consistent of order $p = 1$ in the sense of Definition 4.1.*

Proof. Let $\|\cdot\|_{L^2} := \left(\mathbb{E}[\|\cdot\|^2]\right)^{1/2}$ denote the L^2 -norm. Due to Assumption (A3), the splitting methods (18) and (19) are well-defined. We start with the Lie-Trotter splitting. The triangle inequality yields

$$\left\|\mathbb{E}\left[X_{t_{i-1},x}(t_i) - \tilde{X}_{t_{i-1},x}^{\text{LT}}(t_i)\right]\right\| \leq \left\|\mathbb{E}\left[X_{t_{i-1},x}(t_i) - \tilde{X}_{t_{i-1},x}^{\text{EM}}(t_i)\right]\right\| + \left\|\mathbb{E}\left[\tilde{X}_{t_{i-1},x}^{\text{EM}}(t_i) - \tilde{X}_{t_{i-1},x}^{\text{LT}}(t_i)\right]\right\|$$

and

$$\left\|X_{t_{i-1},x}(t_i) - \tilde{X}_{t_{i-1},x}^{\text{LT}}(t_i)\right\|_{L^2} \leq \left\|X_{t_{i-1},x}(t_i) - \tilde{X}_{t_{i-1},x}^{\text{EM}}(t_i)\right\|_{L^2} + \left\|\tilde{X}_{t_{i-1},x}^{\text{EM}}(t_i) - \tilde{X}_{t_{i-1},x}^{\text{LT}}(t_i)\right\|_{L^2},$$

where $\tilde{X}_{t_{i-1},x}^{\text{EM}}(t_i)$ is the one step-approximation of the Euler-Maruyama scheme (20). Since SDE (1) is of additive noise type, it is known that this method has first order of mean-square consistency [33], i.e., its one-step approximation satisfies

$$\left\|\mathbb{E}[X_{t_{i-1},x}(t_i) - \tilde{X}_{t_{i-1},x}^{\text{EM}}(t_i)]\right\| = \mathcal{O}(\Delta^2), \quad \left\|X_{t_{i-1},x}(t_i) - \tilde{X}_{t_{i-1},x}^{\text{EM}}(t_i)\right\|_{L^2} = \mathcal{O}(\Delta^{3/2}).$$

It remains to consider the difference between the splitting and the Euler-Maruyama method. Using a stochastic Taylor expansion, the solution of the linear stochastic subequation (12) of the splitting framework can be expressed as

$$\varphi_{\Delta}^{[1]}(x) = x + Ax\Delta + \Sigma\sqrt{\Delta}\psi_{i-1} + r, \quad (25)$$

where $r = (r_1, \dots, r_d)^\top$ with $\mathbb{E}[r_j] = \mathcal{O}(\Delta^2)$, $\mathbb{E}[r_j^2] = \mathcal{O}(\Delta^3)$, $j = 1, \dots, d$, and ψ_{i-1} is a Gaussian vector with mean 0_m and covariance matrix \mathbb{I}_m [33]. Similarly, the solution of the ODE subequation (13) of the splitting framework can be expressed as

$$\varphi_{\Delta}^{[2]}(x) = x + N(x)\Delta + q, \quad (26)$$

where the reminder $q = (q_1, \dots, q_d)^\top$ satisfies $q_j = \mathcal{O}(\Delta^2)$, $j = 1, \dots, d$, through a deterministic Taylor expansion. The one-step approximation of the Lie-Trotter splitting method is then obtained by composing the above expressions (25) and (26), yielding

$$\begin{aligned} \tilde{X}_{t_{i-1},x}^{\text{LT}}(t_i) &= (\varphi_{\Delta}^{[1]} \circ \varphi_{\Delta}^{[2]})(x) = x + N(x)\Delta + q \\ &\quad + Ax\Delta + AN(x)\Delta^2 + Aq\Delta + \Sigma\sqrt{\Delta}\varphi_{i-1} + r. \end{aligned}$$

From (20), the one-step approximation of the Euler-Maruyama method is given by

$$\tilde{X}_{t_{i-1},x}^{\text{EM}}(t_i) = x + Ax\Delta + N(x)\Delta + \Sigma\sqrt{\Delta}\psi_{i-1}. \quad (27)$$

Thus, the difference between the Lie-Trotter splitting and the Euler-Maruyama method becomes

$$\tilde{X}_{t_{i-1},x}^{\text{LT}}(t_i) - \tilde{X}_{t_{i-1},x}^{\text{EM}}(t_i) = q + AN(x)\Delta^2 + Aq\Delta + r.$$

Since the stochastic reminders r_j have mean $\mathcal{O}(\Delta^2)$ and second moment $\mathcal{O}(\Delta^3)$, it follows that

$$\left\|\mathbb{E}\left[\tilde{X}_{t_{i-1},x}^{\text{LT}}(t_i) - \tilde{X}_{t_{i-1},x}^{\text{EM}}(t_i)\right]\right\| = \mathcal{O}(\Delta^2) \quad \text{and} \quad \left\|\tilde{X}_{t_{i-1},x}^{\text{LT}}(t_i) - \tilde{X}_{t_{i-1},x}^{\text{EM}}(t_i)\right\|_{L^2} = \mathcal{O}(\Delta^{3/2}),$$

which proves the result for the Lie-Trotter method.

Now, we consider the Strang splitting and define $\omega = (\omega_1, \dots, \omega_d)^\top$ as

$$\omega := N(x)\Delta/2 + q + Ax\Delta + AN(x)\Delta^2/2 + Aq\Delta + \Sigma\sqrt{\Delta}\psi_{i-1} + r,$$

where $\mathbb{E}[\omega_j] = \mathcal{O}(\Delta)$ and $\mathbb{E}[\omega_j^2] = \mathcal{O}(\Delta)$, since $\mathbb{E}[\Delta\psi_{i-1,j}^2] = \Delta$. Applying again a Taylor expansion yields

$$N(x + \omega) = N(x) + \tilde{\omega},$$

where $\tilde{\omega}$ is of same order as ω , i.e., $\mathbb{E}[\tilde{\omega}_j] = O(\Delta)$ and $\mathbb{E}[\tilde{\omega}_j^2] = O(\Delta)$. Using the expressions (25) and (26), the one-step approximation of the Strang splitting method is then given by

$$\begin{aligned}\tilde{X}_{t_{i-1},x}^S(t_i) &= (\varphi_{\Delta/2}^{[2]} \circ \varphi_{\Delta}^{[1]} \circ \varphi_{\Delta/2}^{[2]})(x) = x + \omega + N(x)\Delta/2 + \tilde{\omega}\Delta/2 + q \\ &= x + Ax\Delta + N(x)\Delta + \Sigma\sqrt{\Delta}\psi_{i-1} + 2q + AN(x)\Delta^2/2 + Aq\Delta + r + \tilde{\omega}\Delta/2.\end{aligned}$$

Thus, the difference between the Strang and the Euler-Maruyama method (27) becomes

$$\tilde{X}_{t_{i-1},x}^S(t_i) - \tilde{X}_{t_{i-1},x}^{\text{EM}}(t_i) = 2q + AN(x)\Delta^2/2 + Aq\Delta + r + \tilde{\omega}\Delta/2.$$

Since $\mathbb{E}[r_j] = O(\Delta^2)$, $\Delta\mathbb{E}[\tilde{\omega}_j] = O(\Delta^2)$, $\mathbb{E}[r_j^2] = O(\Delta^3)$ and $\Delta^2\mathbb{E}[\tilde{\omega}_j^2] = O(\Delta^3)$, the result is proved also for the Strang splitting. \square

Now, we establish the boundedness of the second moment of the splitting methods. Intuitively, this is guaranteed by the use of the global explicit solution of the locally Lipschitz ODE (13), which is defined on the entire interval $[0, T]$ without any explosion occurring in finite time. Thus, the iterative composition of this function with the solution of the linear SDE via the Lie-Trotter (18) and Strang (19) methods does not cause an explosion of the moments in finite time either. The proof of this result, however, is not straight-forward. In particular, it requires an assumption related to the locally Lipschitz ODE (13). In Lemma 4.2, we provide two proofs of the mean-square boundedness, each based on a different assumption. The first variant is an extension of the proof of Proposition 3.7 in [9], and is formulated for the Lie-Trotter splitting only. The second variant covers both the Lie-Trotter and the Strang splitting, and builds the basis for the results presented in Section 5.2. The required assumptions are introduced in Assumption 4.1. While the first assumption holds for constant functions $N(x) \equiv c$, and thus linear functions $f(x; \Delta) = c\Delta + x$, this is not the case for the second one. Which of the two proofs is more convenient and which assumption is easier to verify depends on the problem under consideration.

Assumption 4.1. *Let $f : \mathbb{R}^d \rightarrow \mathbb{R}^d$ be as in (17).*

(A4.1) *There exist constants $c_3(\Delta_0) > 0$ and $q \in \mathbb{N}$ such that for any $x \in \mathbb{R}^d$ the auxiliary function*

$$M(x; \Delta) := \frac{f(x; \Delta) - x}{\Delta}$$

satisfies

$$\|M(x; \Delta)\| \leq c_3(\Delta_0) \left(1 + \left\|(|x_1|^{2q}, \dots, |x_d|^{2q})^\top\right\|\right), \quad \forall \Delta \in (0, \Delta_0].$$

(A4.2) *There exists a constant $c_4 \geq 0$ such that for any $x \in \mathbb{R}^d$ it holds that*

$$\|f(x; \Delta)\|^2 \leq \|x\|^2 + c_4\Delta, \quad \forall \Delta \in (0, \Delta_0].$$

Lemma 4.2 (Mean-square boundedness). *Let Assumption (A3) be satisfied and let $\tilde{X}^{LT}(t_i)$ and $\tilde{X}^S(t_i)$ be the Lie-Trotter and Strang splitting defined through (18) and (19), respectively.*

Part I: Let Assumptions (A1) and (A4.1) hold. Then $\tilde{X}^{LT}(t_i)$ is mean-square bounded in the sense of Definition 4.2.

Part II: Let Assumption (A4.2) hold. Then $\tilde{X}^{LT}(t_i)$ and $\tilde{X}^S(t_i)$ are mean-square bounded in the sense of Definition 4.2.

Proof. Due to Assumption (A3), the splitting methods (18) and (19) are well-defined.

Part I: Consider the linear SDE

$$dZ(t) = AZ(t)dt + \Sigma dW(t), \quad Z(0) = Z_0 = 0_d.$$

Its explicit solution is given by

$$Z(t) = \int_0^t e^{A(t-s)} \Sigma dW(s),$$

where $Z(t)$ is normally distributed with mean vector 0_d and covariance matrix $C(t)$ as defined in (15). Consequently, the second moment of $Z(t)$ is bounded, i.e., there exists $C_Z(T) > 0$ such that

$$\mathbb{E} \left[\max_{0 \leq t \leq T} \|Z(t)\|^2 \right] \leq C_Z(T). \quad (28)$$

Moreover, all moments of the components $Z_j(t)$, $j = 1, \dots, d$, of $Z(t)$ are bounded. Thus, for any $p \in \mathbb{N}$ and $j \in \{1, \dots, d\}$, there exists $C_{j,p}(T) > 0$ such that

$$\mathbb{E} \left[\max_{0 \leq t \leq T} |Z_j(t)|^{2p} \right] \leq C_{j,p}(T). \quad (29)$$

Now, define the process $R(t_i) := \tilde{X}^{\text{LT}}(t_i) - Z(t_i)$. Since

$$\left(\sum_{j=1}^l a_j \right)^2 \leq l \sum_{j=1}^l a_j^2,$$

and thus

$$\left\| \tilde{X}^{\text{LT}}(t_i) \right\|^2 = \left\| \tilde{X}^{\text{LT}}(t_i) - Z(t_i) + Z(t_i) \right\|^2 \leq \left(\|R(t_i)\| + \|Z(t_i)\| \right)^2 \leq 2 \|R(t_i)\|^2 + 2 \|Z(t_i)\|^2,$$

the bound (28) implies that it suffices to prove the boundedness of the second moment of the process $R(t_i)$.

Note that in a discretised regime we have that $Z(t_i) = e^{A\Delta} Z(t_{i-1}) + \xi_{i-1}$. Thus,

$$\begin{aligned} \|R(t_i)\| &= \left\| \tilde{X}^{\text{LT}}(t_i) - Z(t_i) \right\| = \left\| e^{A\Delta} \left(f(\tilde{X}^{\text{LT}}(t_{i-1}); \Delta) - Z(t_{i-1}) \right) \right\| \\ &= \left\| e^{A\Delta} \left(f(R(t_{i-1}) + Z(t_{i-1}); \Delta) - Z(t_{i-1}) \right) \right\| \\ &= \left\| e^{A\Delta} \left(f(R(t_{i-1}) + Z(t_{i-1}); \Delta) - f(Z(t_{i-1}); \Delta) + f(Z(t_{i-1}); \Delta) - Z(t_{i-1}) \right) \right\|. \end{aligned}$$

Using that $\|e^{A\Delta} x\| \leq \|e^{A\Delta}\| \|x\| \leq e^{\mu(A)\Delta} \|x\|$ for all $x \in \mathbb{R}^d$, we obtain

$$\|R(t_i)\| \leq e^{\mu(A)\Delta} \|f(R(t_{i-1}) + Z(t_{i-1}); \Delta) - f(Z(t_{i-1}); \Delta)\| + e^{\mu(A)\Delta} \|f(Z(t_{i-1}); \Delta) - Z(t_{i-1})\|.$$

Since the function $N : \mathbb{R}^d \rightarrow \mathbb{R}^d$ satisfies (A1), using the continuous Gronwall Lemma, the function $f : \mathbb{R}^d \rightarrow \mathbb{R}^d$ fulfils the following global Lipschitz condition

$$\|f(x; \Delta) - f(y; \Delta)\| \leq e^{c_1 \Delta} \|x - y\|, \quad \forall x, y \in \mathbb{R}^d,$$

where c_1 is the same as in (A1), see, e.g., [24]. Moreover, noting that $f(x; \Delta) - x = \Delta M(x, \Delta)$ and using Assumption (A4.1), we obtain that

$$\|R(t_i)\| \leq e^{\mu(A)\Delta} \left(e^{c_1 \Delta} \|R(t_{i-1})\| + c_3(\Delta_0) \Delta (1 + \left\| (|Z_1(t_{i-1})|^{2q}, \dots, |Z_d(t_{i-1})|^{2q})^\top \right\|) \right).$$

Defining $\tilde{c} := |\mu(A)| + c_1 > 0$, we get that

$$\|R(t_i)\| \leq e^{\tilde{c}\Delta} \left(\|R(t_{i-1})\| + c_3(\Delta_0) \Delta (1 + \left\| (|Z_1(t_{i-1})|^{2q}, \dots, |Z_d(t_{i-1})|^{2q})^\top \right\|) \right).$$

Now, we can perform back iteration, obtaining

$$\begin{aligned}\|R(t_i)\| &\leq e^{\tilde{c}t_i} \|R_0\| + c_3(\Delta_0) \Delta \sum_{k=1}^i e^{\tilde{c}k\Delta} \left(1 + \left\|(|Z_1(t_{i-k})|^{2q}, \dots, |Z_d(t_{i-k})|^{2q})^\top\right\|\right) \\ &\leq e^{\tilde{c}T} \|X_0\| + c_3(\Delta_0) \left(1 + \max_{0 \leq k \leq i-1} \left\|(|Z_1(t_k)|^{2q}, \dots, |Z_d(t_k)|^{2q})^\top\right\|\right) \Delta \sum_{k=1}^i e^{\tilde{c}k\Delta},\end{aligned}$$

where we used that $R_0 = X_0$, since $Z_0 = 0_d$. Using that

$$\Delta \sum_{k=1}^i e^{\tilde{c}k\Delta} = (e^{\tilde{c}t_i} - 1) \frac{\Delta e^{\tilde{c}\Delta}}{e^{\tilde{c}\Delta} - 1} \leq (e^{\tilde{c}T} - 1) \frac{\Delta_0 e^{\tilde{c}\Delta_0}}{e^{\tilde{c}\Delta_0} - 1}, \quad \forall \Delta \in (0, \Delta_0],$$

we get that

$$\|R(t_i)\| \leq e^{\tilde{c}T} \|X_0\| + c_3(\Delta_0) (e^{\tilde{c}T} - 1) \frac{\Delta_0 e^{\tilde{c}\Delta_0}}{e^{\tilde{c}\Delta_0} - 1} \left(1 + \max_{0 \leq k \leq i-1} \left\|(|Z_1(t_k)|^{2q}, \dots, |Z_d(t_k)|^{2q})^\top\right\|\right).$$

Thus, there exists a constant $C(T, \Delta_0) > 0$ such that

$$\|R(t_i)\| \leq C(T, \Delta_0) \left(1 + \|X_0\| + \max_{0 \leq k \leq i-1} \left\|(|Z_1(t_k)|^{2q}, \dots, |Z_d(t_k)|^{2q})^\top\right\|\right).$$

Moreover, there exists a constant $C_1(T, \Delta_0) > 1$ such that

$$\begin{aligned}\|R(t_i)\|^2 &\leq C_1(T, \Delta_0) \left(1 + \|X_0\| + \max_{0 \leq k \leq i-1} \left\|(|Z_1(t_k)|^{2q}, \dots, |Z_d(t_k)|^{2q})^\top\right\|\right)^2 \\ &\leq 3C_1(T, \Delta_0) \left(1 + \|X_0\|^2 + \max_{0 \leq k \leq i-1} \left\|(|Z_1(t_k)|^{2q}, \dots, |Z_d(t_k)|^{2q})^\top\right\|^2\right) \\ &\leq 3C_1(T, \Delta_0) \left(1 + \|X_0\|^2 + \max_{0 \leq k \leq i-1} |Z_1(t_k)|^{4q} + \dots + \max_{0 \leq k \leq i-1} |Z_d(t_k)|^{4q}\right).\end{aligned}$$

Taking the expectation and using (29) gives

$$\begin{aligned}\mathbb{E} \left[\|R(t_i)\|^2 \right] &\leq 3C_1(T, \Delta_0) \left(1 + \mathbb{E} \left[\|X_0\|^2 \right] + C_{1,2q}(T) + \dots + C_{d,2q}(T) \right) \\ &\leq \tilde{K}(T, \Delta_0) \left(1 + \mathbb{E} \left[\|X_0\|^2 \right] \right).\end{aligned}$$

This concludes the first part of the proof.

Part II: We start with the Lie-Trotter splitting and have that

$$\begin{aligned}\left\| \tilde{X}^{\text{LT}}(t_i) \right\|^2 &= \left\| e^{A\Delta} f(\tilde{X}^{\text{LT}}(t_{i-1}); \Delta) + \xi_{i-1} \right\|^2 \\ &= f(\tilde{X}^{\text{LT}}(t_{i-1}); \Delta)^\top (e^{A\Delta})^\top (e^{A\Delta}) f(\tilde{X}^{\text{LT}}(t_{i-1}); \Delta) \\ &\quad + f(\tilde{X}^{\text{LT}}(t_{i-1}); \Delta)^\top (e^{A\Delta})^\top \xi_{i-1} + \xi_{i-1}^\top e^{A\Delta} f(\tilde{X}^{\text{LT}}(t_{i-1}); \Delta) + \xi_{i-1}^\top \xi_{i-1}.\end{aligned}$$

Taking the expectation, using the fact that $\tilde{X}^{\text{LT}}(t_{i-1})$ and ξ_{i-1} are independent, that $\mathbb{E}[\xi_{i-1}] = 0_d$, that $\mathbb{E}[\xi_{i-1}^\top] = 0_d^\top$ and that

$$\bar{C}(\Delta) := \sum_{j=1}^d c_{jj}(\Delta) = \mathbb{E}[\xi_{i-1}^\top \xi_{i-1}],$$

we get that

$$\begin{aligned}\mathbb{E} \left[\left\| \tilde{X}^{\text{LT}}(t_i) \right\|^2 \right] &= \mathbb{E} \left[f(\tilde{X}^{\text{LT}}(t_{i-1}); \Delta)^\top (e^{A\Delta})^\top (e^{A\Delta}) f(\tilde{X}^{\text{LT}}(t_{i-1}); \Delta) \right] + \bar{C}(\Delta) \\ &= \mathbb{E} \left[\left\| e^{A\Delta} f(\tilde{X}^{\text{LT}}(t_{i-1}); \Delta) \right\|^2 \right] + \bar{C}(\Delta).\end{aligned}\tag{30}$$

Using Assumption (A4.2) and the logarithmic norm, we further obtain

$$\mathbb{E} \left[\left\| \tilde{X}^{\text{LT}}(t_i) \right\|^2 \right] \leq e^{2\mu(A)\Delta} \left(\mathbb{E} \left[\left\| \tilde{X}^{\text{LT}}(t_{i-1}) \right\|^2 \right] + c_4 \Delta \right) + \bar{C}(\Delta).$$

Now, we can perform back iteration, yielding

$$\mathbb{E} \left[\left\| \tilde{X}^{\text{LT}}(t_i) \right\|^2 \right] \leq e^{2\mu(A)t_i} \mathbb{E} \left[\|X_0\|^2 \right] + c_4 \Delta \sum_{k=1}^i e^{2\mu(A)k\Delta} + \bar{C}(\Delta) \sum_{k=0}^{i-1} e^{2\mu(A)k\Delta}.$$

Using that

$$\begin{aligned} \sum_{k=1}^i e^{2\mu(A)k\Delta} &= \left(1 - e^{2\mu(A)t_i}\right) \frac{e^{2\mu(A)\Delta}}{(1 - e^{2\mu(A)\Delta})}, \\ \sum_{k=0}^{i-1} e^{2\mu(A)k\Delta} &= \left(1 - e^{2\mu(A)t_i}\right) \frac{1}{(1 - e^{2\mu(A)\Delta})}, \end{aligned}$$

we obtain

$$\mathbb{E} \left[\left\| \tilde{X}^{\text{LT}}(t_i) \right\|^2 \right] \leq e^{2\mu(A)t_i} \mathbb{E} \left[\|X_0\|^2 \right] + \left(1 - e^{2\mu(A)t_i}\right) \left(\frac{c_4 \Delta e^{2\mu(A)\Delta}}{1 - e^{2\mu(A)\Delta}} + \frac{\bar{C}(\Delta)}{1 - e^{2\mu(A)\Delta}} \right), \quad (31)$$

where $e^{2\mu(A)t_i}$ and $(1 - e^{2\mu(A)t_i})$ can be bounded by $e^{2|\mu(A)|T}$ and $(1 + e^{2|\mu(A)|T})$, respectively. Moreover, we have that

$$\frac{\Delta e^{2\mu(A)\Delta}}{1 - e^{2\mu(A)\Delta}} \leq -\frac{1}{2\mu(A)}, \quad \forall \Delta > 0 \quad \text{and} \quad \frac{\Delta}{1 - e^{2\mu(A)\Delta}} \leq \frac{\Delta_0}{1 - e^{2\mu(A)\Delta_0}}, \quad \forall \Delta \in (0, \Delta_0]. \quad (32)$$

Recalling that $e^{A\Delta} = \mathbb{I}_d + \Delta A + O(\Delta^2)$, it follows from (15) that $\bar{C}(\Delta) = O(\Delta)$. Thus, there exists a constant $\tilde{K}(T, \Delta_0)$ such that

$$\mathbb{E} \left[\left\| \tilde{X}^{\text{LT}}(t_i) \right\|^2 \right] \leq \tilde{K}(T, \Delta_0) \left(1 + \mathbb{E} \left[\|X_0\|^2 \right] \right).$$

This proves the result for the Lie-Trotter splitting.

Now, we consider the Strang splitting and note that

$$\begin{aligned} \left\| \tilde{X}^{\text{S}}(t_i) \right\|^2 &= \left\| f \left(e^{A\Delta} f(\tilde{X}^{\text{S}}(t_{i-1}); \Delta/2) + \xi_{i-1}; \Delta/2 \right) \right\|^2 \\ &\leq \left\| e^{A\Delta} f(\tilde{X}^{\text{S}}(t_{i-1}); \Delta/2) + \xi_{i-1} \right\|^2 + c_4 \Delta/2, \end{aligned} \quad (33)$$

using Assumption (A4.2). Proceeding in the same way as for the Lie-Trotter splitting, we obtain

$$\mathbb{E} \left[\left\| \tilde{X}^{\text{S}}(t_i) \right\|^2 \right] \leq e^{2\mu(A)t_i} \mathbb{E} \left[\|X_0\|^2 \right] + \left(1 - e^{2\mu(A)t_i}\right) \left(\frac{c_4 \Delta/2(1 + e^{2\mu(A)\Delta})}{1 - e^{2\mu(A)\Delta}} + \frac{\bar{C}(\Delta)}{1 - e^{2\mu(A)\Delta}} \right). \quad (34)$$

Using the same arguments as before, the result is also proved for the Strang splitting. This concludes the second part of the proof. \square

Based on the above results, we establish the mean-square convergence of the splitting methods in the following theorem.

Theorem 4.2 (Mean-square convergence). *Let $\tilde{X}^{LT}(t_i)$ and $\tilde{X}^S(t_i)$ be the Lie-Trotter and Strang splitting defined through (18) and (19), respectively. Further, let the assumptions of Theorem 4.1, Lemma 4.1 and Lemma 4.2 be satisfied. Then $\tilde{X}^{LT}(t_i)$ and $\tilde{X}^S(t_i)$ are mean-square convergent of order $p = 1$ in the sense of (2).*

Proof. The result is a direct consequence of Theorem 4.1, Lemma 4.1 and Lemma 4.2. \square

Note that, in contrast to deterministic equations [20], the convergence order of a splitting method cannot be increased by using compositions based on fractional steps. Indeed, to achieve this in the stochastic scenario, higher-order stochastic integrals would be required [44]. Thus, the Strang method (19) has also mean-square order 1. Nevertheless, it has been observed that, even without including higher-order stochastic integrals, the Strang approach may perform considerably better than the Lie-Trotter method in numerical experiments, see, e.g., [2, 10, 11, 12, 64], possibly due to the symmetry of this composition method.

5 Structure preservation

The mean-square convergence discussed in the previous section is a limit result for the time discretisation step Δ going to zero over a finite interval. This result does not carry any information about the quality of the numerical method under the use of strictly positive time steps Δ , as always required when implementing any numerical method. In the following, we discuss the preservation of important structural properties. In particular, we focus on hypoellipticity and ergodicity.

5.1 Preservation of noise structure and 1-step hypoellipticity

To obtain a discrete analogue of the transition probability (3) introduced in Section 2, we define the k -step transition probability of a numerical solution $\tilde{X}(t_i)$ of SDE (1) as follows

$$\tilde{P}_{t_k}(\mathcal{A}, x) := \mathbb{P}(\tilde{X}(t_k) \in \mathcal{A} | X(0) = x), \quad (35)$$

where $\mathcal{A} \in \mathcal{B}(\mathbb{R}^d)$ and $x \in \mathbb{R}^d$. Now, assume that SDE (1) is hypoelliptic, i.e., its transition probability (3) has a smooth density even though $\Sigma\Sigma^\top$ is not of full rank. A discrete version of this property is provided in the subsequent definition.

Definition 5.1 (k -step hypoellipticity). *Let $\tilde{X}(t_i)$ be a numerical solution of (1) and $k \in \mathbb{N}$ be the smallest k such that its transition probability (35) has a smooth density. Then, $\tilde{X}(t_i)$ is called k -step hypoelliptic.*

This means that the numerical method propagates the noise into the smooth component after k iteration steps. The preservation of this property is not an issue when using the numerical method to simulate paths of the SDE over a large enough time horizon, as standard methods usually satisfy it for some k . For example, Euler-Maruyama type methods have been observed to be 2-step hypoelliptic, see, e.g., Corollary 7.4 in [40].

However, the case $k = 1$, where we also use the notation

$$\tilde{P}_\Delta(\mathcal{A}, x) := \mathbb{P}(\tilde{X}(t_i) \in \mathcal{A} | \tilde{X}(t_{i-1}) = x), \quad (36)$$

is of crucial relevance when using the numerical method within statistical applications. In the following, we provide a brief insight into this issue. In the field of likelihood-based parameter estimation [17, 42, 52], a particular interest lies in the situation where (36) corresponds to the multivariate normal distribution, i.e., $\tilde{X}(t_i)$ given $\tilde{X}(t_{i-1})$ is normally distributed with mean vector and covariance matrix given by

$$\mathbb{E} \left[\tilde{X}(t_i) | \tilde{X}(t_{i-1}) \right] = m_i(\tilde{X}(t_{i-1}), \Delta; \theta), \quad \text{Cov} \left(\tilde{X}(t_i) | \tilde{X}(t_{i-1}) \right) = Q(\Delta; \theta),$$

respectively, where θ denotes the relevant model parameters which are aimed to be inferred, based on discrete time observations of the process $(\tilde{X}(t))_{t \in [0, T]}$. Assuming that the process is fully observed and that $(x(t_i))_{i=0, \dots, n}$ are the available data, the estimator of θ can be obtained as

$$\arg \min_{\theta} \sum_{i=1}^n \left[(x(t_i) - m_i(x(t_{i-1}), \Delta; \theta))^{\top} Q(\Delta; \theta)^{-1} (x(t_i) - m_i(x(t_{i-1}), \Delta; \theta)) \right] + n \log(\det(Q(\Delta; \theta))),$$

a criterion which results from taking minus two times the corresponding log-likelihood. This estimation tool is only well-defined if $Q(\Delta; \theta)^{-1}$ exists and $\det(Q(\Delta; \theta)) > 0$, i.e., if the underlying numerical method $\tilde{X}(t_i)$ is 1-step hypoelliptic.

This is not fulfilled by Euler-Maruyama type methods. For example, (20), (21) and (23) yield degenerate multivariate normal distributions with non-invertible conditional covariance matrices

$$\begin{aligned} \text{Cov}(\tilde{X}^{\text{EM}}(t_i) | \tilde{X}^{\text{EM}}(t_{i-1})) &= \text{Cov}(\tilde{X}^{\text{TEM}}(t_i) | \tilde{X}^{\text{TEM}}(t_{i-1})) \\ &= \text{Cov}(\tilde{X}^{\text{TrEM}}(t_i) | \tilde{X}^{\text{TrEM}}(t_{i-1})) = \Delta \Sigma \Sigma^{\top}. \end{aligned}$$

Thus, they do not have a density and are impracticable within statistical inference tools for hypoelliptic SDEs. In contrast, the splitting methods benefit from the random quantities ξ_i which have covariance matrix $C(\Delta)$, as defined in (15). Both the diffusion matrix Σ and the drift matrix A , through its exponential, enter into $C(\Delta)$. Thus, the splitting methods are 1-step hypoelliptic provided that the stochastic linear subequation (12) of the splitting framework is hypoelliptic. While the conditional distribution of the Strang splitting is not explicitly available in general, the Lie-Trotter method yields a non-degenerate multivariate normal distribution.

Theorem 5.1. *Let Assumption (A3) hold and let $\tilde{X}^{LT}(t_i)$ be the Lie-Trotter splitting defined through (18). Further, assume that SDE (12) is hypoelliptic. Then, $\tilde{X}^{LT}(t_i)$ is 1-step hypoelliptic according to Definition 5.1. Moreover, $\tilde{X}^{LT}(t_i)$ given $\tilde{X}^{LT}(t_{i-1})$ admits a non-degenerate normal distribution with mean vector and covariance matrix given by*

$$\mathbb{E} \left[\tilde{X}^{LT}(t_i) | \tilde{X}^{LT}(t_{i-1}) \right] = e^{A\Delta} f(\tilde{X}^{LT}(t_{i-1}); \Delta), \quad \text{Cov}(\tilde{X}^{LT}(t_i) | \tilde{X}^{LT}(t_{i-1})) = C(\Delta),$$

respectively, where $C(\Delta)$ is defined in (15).

Proof. Due to Assumption (A3), the Lie-Trotter splitting (18) is well-defined. The fact that $\tilde{X}^{LT}(t_i)$ given $\tilde{X}^{LT}(t_{i-1})$ is normally distributed with the corresponding mean vector and covariance matrix is an immediate consequence of formula (18), recalling that ξ_i are Gaussian random vectors with null mean and covariance matrix $C(\Delta)$. Moreover, the linear SDE (12) is hypoelliptic by assumption. Thus, its solution $(X^{[1]}(t))_{t \in [0, T]}$ has conditional covariance matrix $C(t) = \text{Cov}(X^{[1]}(t) | X_0^{[1]})$ (15) which is of full rank. Since the covariance matrix of the Lie-Trotter splitting equals $C(\Delta)$, this method is 1-step hypoelliptic according to Definition 5.1, and thus the normal distribution is non-degenerate. \square

5.2 Preservation of Lyapunov structure and geometric ergodicity

We now assume that SDE (1) is geometrically ergodic. The main task to establish the geometric ergodicity of a numerical solution of (1) is to prove a discrete analogue of the Lyapunov condition (7) introduced in Section 2.

Definition 5.2 (Discrete Lyapunov condition). *Let L be a Lyapunov function for SDE (1). A numerical solution $\tilde{X}(t_i)$ of (1) satisfies the discrete Lyapunov condition if there exist $\tilde{\rho} \in (0, 1)$ and $\tilde{\eta} > 0$ such that*

$$\mathbb{E} \left[L(\tilde{X}(t_i)) | \tilde{X}(t_{i-1}) \right] \leq \tilde{\rho} L(\tilde{X}(t_{i-1})) + \tilde{\eta}, \quad \forall i \in \mathbb{N}.$$

Analogously to the continuous case, this condition, combined with the k -step hypoellipticity and a discrete irreducibility condition, implies geometric ergodicity of the numerical method. For further details, the reader is referred to [2, 40].

Unfortunately, Euler-Maruyama type methods do not preserve this property, especially when the drift of SDE (1) is only locally Lipschitz continuous. In particular, the problem does not lie in the preservation of hypoellipticity and irreducibility, but in preserving the Lyapunov structure [40]. Consider, for example, the cubic one-dimensional SDE

$$dX(t) = -X^3(t)dt + \sigma dW(t), \quad X(0) = X_0. \quad (37)$$

Since $F(x)x = -x^4 \leq 1 - x^4 \leq 2 - 2x^2$, this SDE satisfies the dissipativity condition (6), and thus $L(x) = 1 + x^2$ is a Lyapunov function satisfying (7) and the process $(X(t))_{t \in [0, T]}$ is geometrically ergodic. However, it is shown in Lemma 6.3 of [40] that, if $\mathbb{E}[X_0^2] \geq 2/\Delta$, the second moment of the Euler-Maruyama method goes to infinity as the time t_i grows, since

$$\mathbb{E} \left[\left(\tilde{X}^{\text{EM}}(t_i) \right)^2 \right] \geq \mathbb{E}[X_0^2] + t_i.$$

Thus, even for arbitrarily small time steps Δ , the Euler-Maruyama method fails to converge to a unique invariant distribution independently of the choice of X_0 .

In contrast, splitting methods often preserve the Lyapunov structure, see, e.g., [2, 12]. This is also proved for the proposed splitting methods and the Lyapunov function $L(x) = 1 + \|x\|^2$, under Assumption (A4.2) and an additional assumption related to the matrix A .

Assumption 5.1. (A5) *The matrix A is such that $\|e^{A\Delta}\| < 1$ for all $\Delta \in (0, \Delta_0]$.*

Theorem 5.2. *Let Assumption (A3) hold and let $\tilde{X}^{\text{LT}}(t_i)$ and $\tilde{X}^{\text{S}}(t_i)$ be the Lie-Trotter and Strang splitting defined through (18) and (19), respectively. Further, suppose that $L(x) = 1 + \|x\|^2$ is a Lyapunov function of SDE (1) and that Assumptions (A4.2) and (A5) are satisfied. Then $\tilde{X}^{\text{LT}}(t_i)$ and $\tilde{X}^{\text{S}}(t_i)$ satisfy the discrete Lyapunov condition of Definition 5.2.*

Proof. Due to Assumption (A3), the splitting methods (18) and (19) are well-defined. We start with the Lie-Trotter splitting and have that

$$L(\tilde{X}^{\text{LT}}(t_i)) = 1 + \left\| \tilde{X}^{\text{LT}}(t_i) \right\|^2 = 1 + \left\| e^{A\Delta} f(\tilde{X}^{\text{LT}}(t_{i-1}); \Delta) + \xi_{i-1} \right\|^2.$$

Using (30) and Assumption (A4.2), we get that

$$\begin{aligned} \mathbb{E} \left[L(\tilde{X}^{\text{LT}}(t_i)) | \tilde{X}^{\text{LT}}(t_{i-1}) \right] &= 1 + \left\| e^{A\Delta} f(\tilde{X}^{\text{LT}}(t_{i-1}); \Delta) \right\|^2 + \bar{C}(\Delta) \\ &\leq 1 + \|e^{A\Delta}\|^2 \left\| \tilde{X}^{\text{LT}}(t_{i-1}) \right\|^2 + \|e^{A\Delta}\|^2 c_4 \Delta + \bar{C}(\Delta) + \|e^{A\Delta}\|^2 \\ &= \|e^{A\Delta}\|^2 L(\tilde{X}^{\text{LT}}(t_{i-1})) + 1 + \|e^{A\Delta}\|^2 c_4 \Delta + \bar{C}(\Delta), \end{aligned}$$

where we added $\|e^{A\Delta}\|^2$ in the inequality. Thus, applying Assumption (A5), the discrete Lyapunov condition of Definition 5.2 is satisfied for $\tilde{\rho} = \|e^{A\Delta}\|^2 < 1$ and $\tilde{\eta} = 1 + \|e^{A\Delta}\|^2 c_4 \Delta + \bar{C}(\Delta) > 0$.

Now, we consider the Strang splitting. Using (33), we get that

$$L(\tilde{X}^{\text{S}}(t_i)) = 1 + \left\| \tilde{X}^{\text{S}}(t_i) \right\|^2 \leq 1 + \left\| e^{A\Delta} f(\tilde{X}^{\text{S}}(t_{i-1}); \Delta/2) + \xi_{i-1} \right\|^2 + c_4 \Delta/2.$$

Starting from here, the result for the Strang splitting can be proved in the same way as for the Lie-Trotter splitting. In particular, the condition of Definition 5.2 holds for $\tilde{\rho} = \|e^{A\Delta}\|^2 < 1$ and $\tilde{\eta} = 1 + \|e^{A\Delta}\|^2 c_4 \Delta/2 + \bar{C}(\Delta) + c_4 \Delta/2 > 0$. \square

Moreover, in the following corollary of Lemma 4.2 (Part II), we show that the second moments of the splitting methods are asymptotically bounded by constants which are independent of T and Δ . In particular, these bounds are reached exponentially fast, independently of the choice of X_0 , in agreement with the geometric ergodicity of the splitting methods. This result also requires Assumption (A4.2) and an assumption related to the matrix A .

Assumption 5.2. (A6) *The matrix A is such that the logarithmic norm $\mu(A) < 0$.*

Note that Assumption (A6) implies Assumption (A5), since $\|e^{A\Delta}\| \leq e^{\mu(A)\Delta}$ [60]. However, the converse is not true in general. Assumption (A6) is, e.g., satisfied for normal matrices, where all eigenvalues have strictly negative real part [58]. Matrices contained in this class are, e.g., diagonal ones with strictly negative diagonal entries.

Corollary 5.1. *Let Assumption (A3) hold and let $\tilde{X}^{LT}(t_i)$ and $\tilde{X}^S(t_i)$ be the Lie-Trotter and Strang splitting defined through (18) and (19), respectively. Further, let Assumptions (A4.2) and (A6) be satisfied. Then there exist constant $\tilde{K}_\infty^{LT}(\Delta_0) > 0$ and $\tilde{K}_\infty^S(\Delta_0) > 0$, which are independent of T and Δ , such that*

$$\lim_{t_i \rightarrow \infty} \mathbb{E} \left[\left\| \tilde{X}^{LT}(t_i) \right\|^2 \right] \leq \tilde{K}_\infty^{LT}(\Delta_0), \quad \lim_{t_i \rightarrow \infty} \mathbb{E} \left[\left\| \tilde{X}^S(t_i) \right\|^2 \right] \leq \tilde{K}_\infty^S(\Delta_0).$$

Proof. Recall the bounds (31) and (34) from the proof of Part II of Lemma 4.2, which can be derived under Assumption (A4.2). Applying Assumption (A6), we further obtain that

$$\begin{aligned} \lim_{t_i \rightarrow \infty} \mathbb{E} \left[\left\| \tilde{X}^{LT}(t_i) \right\|^2 \right] &\leq \frac{c_4 \Delta e^{2\mu(A)\Delta}}{1 - e^{2\mu(A)\Delta}} + \frac{\bar{C}(\Delta)}{1 - e^{2\mu(A)\Delta}}, \\ \lim_{t_i \rightarrow \infty} \mathbb{E} \left[\left\| \tilde{X}^S(t_i) \right\|^2 \right] &\leq \frac{c_4}{2} \left(\frac{\Delta}{1 - e^{2\mu(A)\Delta}} + \frac{\Delta e^{2\mu(A)\Delta}}{1 - e^{2\mu(A)\Delta}} \right) + \frac{\bar{C}(\Delta)}{1 - e^{2\mu(A)\Delta}}. \end{aligned}$$

Using (32), and the fact that $\bar{C}(\Delta) = O(\Delta)$, the result holds. \square

The one-dimensional case In the one-dimensional case, the previously derived bounds have convenient closed-form expressions, due to the specific form of the covariance matrix $C(\Delta)$. In particular, the bounds for the Lie-Trotter splitting no longer depend on Δ_0 . The following (asymptotic) bounds for the second moment of the splitting methods are obtained.

Corollary 5.2. *Let Assumption (A3) hold and let $\tilde{X}^{LT}(t_i)$ and $\tilde{X}^S(t_i)$ be the Lie-Trotter and Strang splitting defined through (18) and (19), respectively. Further, let Assumption (A4.2) be satisfied, $d = 1$, $\Sigma = \sigma > 0$ and $A = -a < 0$. Then it holds that*

$$\begin{aligned} \mathbb{E} \left[(\tilde{X}^{LT}(t_i))^2 \right] &\leq \tilde{K}^{LT}(t_i, X_0) := e^{-2at_i} \mathbb{E} [X_0^2] + (1 - e^{-2at_i}) \left(\frac{c_4}{2a} + \frac{\sigma^2}{2a} \right), \\ \mathbb{E} \left[(\tilde{X}^S(t_i))^2 \right] &\leq \tilde{K}^S(t_i, X_0, \Delta_0) \\ &:= e^{-2at_i} \mathbb{E} [X_0^2] + (1 - e^{-2at_i}) \left(\frac{c_4}{2} \left(\frac{\Delta_0}{1 - e^{-2a\Delta_0}} + \frac{1}{2a} \right) + \frac{\sigma^2}{2a} \right), \\ \lim_{t_i \rightarrow \infty} \mathbb{E} \left[(\tilde{X}^{LT}(t_i))^2 \right] &\leq \tilde{K}_\infty^{LT} := \frac{c_4}{2a} + \frac{\sigma^2}{2a}, \\ \lim_{t_i \rightarrow \infty} \mathbb{E} \left[(\tilde{X}^S(t_i))^2 \right] &\leq \tilde{K}_\infty^S(\Delta_0) := \frac{c_4}{2} \left(\frac{\Delta_0}{1 - e^{-2a\Delta_0}} + \frac{1}{2a} \right) + \frac{\sigma^2}{2a}. \end{aligned}$$

Proof. Noting that

$$\bar{C}(\Delta) = C(\Delta) = \frac{\sigma^2}{2a} (1 - e^{-2a\Delta}) \quad \text{and} \quad \mu(A) = -a < 0,$$

the result is a direct consequence of Part II of Lemma 4.2 (using (31), (32) and (34)) and Corollary 5.1. \square

Remark 5.1. For $t_i = 0$, the bounds $\tilde{K}^{LT}(0, X_0)$ and $\tilde{K}^S(0, X_0, \Delta_0)$ in Corollary 5.2 coincide with $\mathbb{E}[X_0^2]$. Moreover, $\tilde{K}^S(t_i, X_0, \Delta_0)$ and $\tilde{K}_\infty^S(\Delta_0)$ approach $\tilde{K}^{LT}(t_i, X_0)$ and \tilde{K}_∞^{LT} , respectively, as Δ_0 tends to zero.

Note that, since $a > 0$, the linear SDE (12) is geometrically ergodic. In particular, its solution corresponds to the Ornstein-Uhlenbeck process

$$X^{[1]}(t) = e^{-at} X_0^{[1]} + \sigma \int_0^t e^{-a(t-s)} dW(s),$$

whose distribution converges to a unique limit

$$X^{[1]}(t) \xrightarrow[t \rightarrow \infty]{\mathcal{D}} \mathcal{N}(0, \frac{\sigma^2}{2a}).$$

Intuitively, this fact, combined with Assumption (A4.2), guarantees the geometric ergodicity of the splitting methods obtained via Theorem 5.2, and thus the existence of the asymptotic bounds for the second moment.

Cubic model problem For an illustration of the derived bounds, consider again SDE (37). We propose to rewrite this equation as

$$dX(t) = (-X(t) + X(t) - X^3(t)) dt + \sigma dW(t),$$

and to choose

$$A = -1 < 0, \quad N(X(t)) = X(t) - X^3(t). \quad (38)$$

Assumptions (A1) and (A2) regarding the function N hold.

Proposition 5.1. Let $N : \mathbb{R} \rightarrow \mathbb{R}$ be as in (38). Then N satisfies Assumptions (A1) and (A2).

Proof. The proof is given in Appendix A. \square

The global explicit solution of ODE (13) exists and is given by

$$X^{[2]}(t) = f(X_0^{[2]}; t) = \frac{X_0^{[2]}}{\sqrt{e^{-2t} + (X_0^{[2]})^2(1 - e^{-2t})}}. \quad (39)$$

Thus, Assumption (A3) is satisfied and the Lie-Trotter (18) and Strang (19) splitting methods are well-defined. In addition, Assumption (A4.1) can be proved in the same way as Lemma 3.4 in [9], and Assumption (A4.2) is proved as follows.

Proposition 5.2. Let $f : \mathbb{R} \rightarrow \mathbb{R}$ be as in (39). Then f satisfies Assumption (A4.2) for $c_4 = 1/2$.

Proof. The proof is given in Appendix B. \square

Note also that Assumptions (A5) and (A6) regarding A hold, since $\|e^{A\Delta}\| = e^{-\Delta} < 1$ and $\mu(A) = -1 < 0$. Therefore, the splitting methods (18) and (19) applied to SDE (37) are not only mean-square convergent, but also geometrically ergodic. In particular, while even for arbitrarily small Δ one can find X_0 such that the second moment of the Euler-Maruyama method explodes (see the beginning of Section 5.2), the second moments of the splitting methods are bounded by the constants $\tilde{K}^{LT}(t_i, X_0)$ and $\tilde{K}^S(t_i, X_0, \Delta_0)$, which converge exponentially fast to

$$\tilde{K}_\infty^{LT} = \frac{1}{4} + \frac{\sigma^2}{2} \quad \text{and} \quad \tilde{K}_\infty^S(\Delta_0) = \frac{1}{4} \left(\frac{\Delta_0}{1 - e^{-2\Delta_0}} + \frac{1}{2} \right) + \frac{\sigma^2}{2},$$

for any choice of the initial value X_0 , see Corollary 5.2.

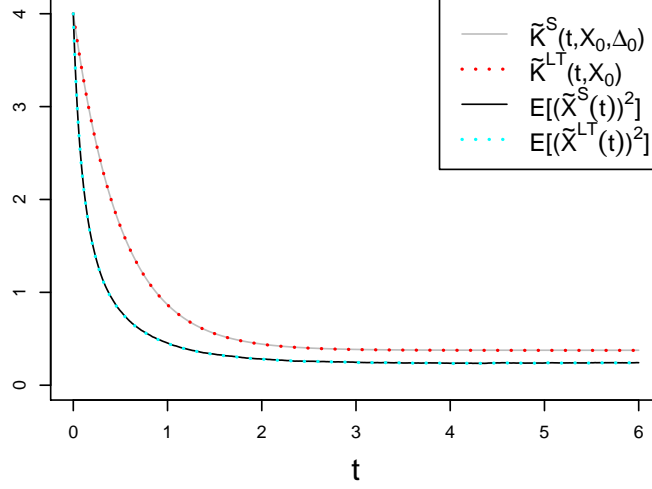


Figure 1: Bounds $\tilde{K}^S(t_i, X_0, \Delta_0)$ and $\tilde{K}^{LT}(t_i, X_0)$ of Corollary 5.2 for SDE (37) ($a = 1$ and $c_4 = 1/2$) with $\sigma = 1/2$, $X_0 = 2$ and $\Delta_0 = 10^{-2}$ as functions of time, and estimates of $\mathbb{E}[X^2(t)]$ obtained from 10^4 paths generated under the LT and S splittings, respectively.

In Figure 1, we illustrate the derived bounds $\tilde{K}^S(t_i, X_0, \Delta_0)$ (grey solid line) and $\tilde{K}^{LT}(t_i, X_0)$ (red dotted line) of Corollary 5.2 for SDE (37). The bounds are almost overlapping for $\Delta_0 = 10^{-2}$ and converge to \tilde{K}_∞^{LT} and $\tilde{K}_\infty^S(\Delta_0)$, respectively, as t grows. Moreover, we estimate $\mathbb{E}[X^2(t)]$ based on 10^4 paths generated under the Strang (19) (black solid line) and Lie-Trotter (18) (cyan dotted line) splitting, respectively. Both estimates almost overlap and lie below the bound. They also converge to a constant, which is smaller than \tilde{K}_∞^{LT} and $\tilde{K}_\infty^S(\Delta_0)$, as the time evolves.

Remark 5.2. For SDE (37), an immediate choice of the subequations of the splitting framework would also be $N(X(t)) = -X^3(t)$ and $A = 0$. For this choice, Assumptions (A1)-(A4.2) related to the locally Lipschitz function N are satisfied, and thus the resulting splitting methods (18) and (19) are mean-square convergent. However, since $e^{A\Delta} = 1$ and $\mu(A) = 0$, Assumptions (A5) and (A6) do not hold, asymptotic bounds cannot be derived, and the preservation of ergodicity remains an open question. In particular, in contrast to the proposed approach, the distribution of the solution of the resulting linear SDE does not converge to a unique limit, and thus SDE (12) is not ergodic.

In the following, we illustrate how the choice of X_0 influences the behaviour of paths of the ergodic process $X(t)$ simulated under the different numerical methods. If X_0 is large, the Euler-Maruyama method produces paths which are computationally pushed to $+/-$ infinity within a few iteration steps, even for very small values of Δ . This is not the case for the tamed/truncated variants of this method. However, when X_0 is large, they may also react sensitively to X_0 , even for small Δ . This is illustrated in Figure 2, where we report paths of SDE (37) generated for $X_0 = 10^4$ (left panel) and $X_0 = 3 \cdot 10^4$ (right panel), using $\Delta = 10^{-4}$ and $\sigma = 1/2$. The grey reference paths are simulated under $\Delta = 10^{-7}$ using the TEM method (21). The choice of the reference method does not change the reported results. Moreover, all paths are generated under the same underlying pseudo random numbers. As desired, the paths obtained under the splitting methods are not deterred by the large value of X_0 , and overlap with the reference path. In contrast, the Euler-Maruyama type methods introduce a delay in when the respective paths reach the reference path. This behaviour deteriorates as X_0 increases. A similar picture is obtained for larger values of Δ and accordingly smaller values of X_0 . Moreover, for some values of X_0 , we observe that the DTrEM method (24) may produce spurious oscillations (figures not shown). See [30, 62], where such a behaviour has also been observed.

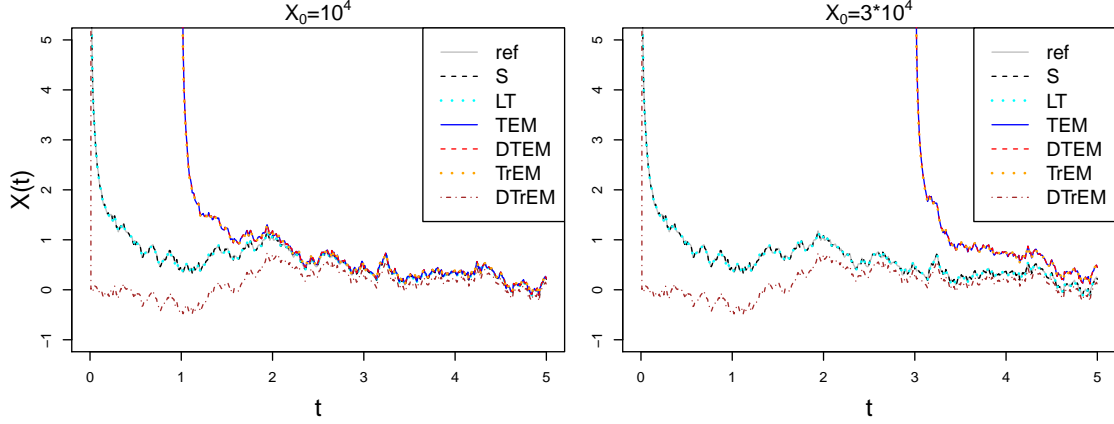


Figure 2: Paths of SDE (37) simulated under the considered numerical methods for large values of X_0 , $\Delta = 10^{-4}$ and $\sigma = 1/2$. The grey reference paths are obtained under $\Delta = 10^{-7}$ using the TEM method (21).

6 Stochastic FitzHugh-Nagumo model

In this section, the proposed splitting methods are illustrated on the stochastic FHN model, a widely used neuronal model. It is given by the following 2-dimensional SDE

$$d \begin{pmatrix} V(t) \\ U(t) \end{pmatrix} = \underbrace{\begin{pmatrix} \frac{1}{\epsilon} (V(t) - V^3(t) - U(t)) \\ \gamma V(t) - U(t) + \beta \end{pmatrix}}_{:= F(X(t))} dt + \underbrace{\begin{pmatrix} \sigma_1 & 0 \\ 0 & \sigma_2 \end{pmatrix}}_{:= \Sigma} dW(t), \quad X(0) = X_0, \quad t \in [0, T], \quad (40)$$

with solution $X(t) := (V(t), U(t))^\top$ for $t \in [0, T]$. This equation has been used to model the firing activity of single neurons [18, 49]. If the membrane voltage of the neuron is sufficiently high, it releases an action potential, also called spike. The first component $(V(t))_{t \in [0, T]}$ describes the membrane voltage of the neuron at time t , while the second component $(U(t))_{t \in [0, T]}$ corresponds to a recovery variable modelling the channel kinetics. The parameter $\epsilon > 0$ corresponds to the time scale separation of the two components and $\beta \geq 0$ and $\gamma > 0$ are position and duration parameters of an excitation, respectively. SDE (40) could be extended by adding a parameter, modelling an injected input current, to the first component of the drift. This parameter is typically set to zero, see, e.g., [17, 36, 13], and thus neglected here. If it is not zero, a splitting method which considers a third subequation could be derived.

Properties of the FHN model If both noise intensities σ_1 and σ_2 are strictly positive, the model is elliptic. If $\sigma_1 = 0$, the diffusion term becomes $\Sigma dW(t) = (0, \sigma_2)^\top dW_2(t)$, corresponding to the notation in (4). In this case, due to the U -component entering the first entry of the drift $F(X(t))$, the model is hypoelliptic. This is confirmed by the fact that

$$\partial_u F_1(x) \sigma_2 = -\frac{\sigma_2}{\epsilon} \neq 0, \quad (41)$$

guaranteeing Condition (5). We refer to [5, 7, 30, 48] and to [17, 36] for the consideration of the elliptic and hypoelliptic FHN model, respectively, and to [13] for an investigation of both cases.

Moreover, it has been proved that the FHN model is ergodic, see, e.g., [7, 36]. Here, we study this property under a restricted parameter space, for which SDE (40) satisfies the dissipativity condition (6) such that the function $L(x) = 1 + \|x\|^2$ is a Lyapunov function meeting Condition (7).

Proposition 6.1. *Let*

$$\frac{1}{\epsilon} > \frac{1}{2} \left| \gamma - \frac{1}{\epsilon} \right| \quad \text{and} \quad 1 - \beta > \frac{1}{2} \left| \gamma - \frac{1}{\epsilon} \right|.$$

Then, the drift F of the FHN model (40) satisfies the dissipativity condition (6).

Proof. We have that

$$(F(x), x) = \left(\begin{pmatrix} \frac{1}{\epsilon}(v - v^3 - u) \\ \gamma v - u + \beta \end{pmatrix}, \begin{pmatrix} v \\ u \end{pmatrix} \right) = \frac{1}{\epsilon}(v^2 - v^4) + vu(\gamma - \frac{1}{\epsilon}) - u^2 + \beta u.$$

Defining $c := |\gamma - 1/\epsilon|$ and using $2vu \leq v^2 + u^2$, $u < 1 + u^2$ and $v^2 - v^4 \leq 1 - v^2$, we obtain

$$\begin{aligned} (F(x), x) &\leq \frac{1}{\epsilon}(1 - v^2) + \frac{c}{2}(v^2 + u^2) - u^2 + \beta(1 + u^2) \\ &= -v^2\left(\frac{1}{\epsilon} - \frac{c}{2}\right) - u^2\left(1 - \beta - \frac{c}{2}\right) + \beta + \frac{1}{\epsilon}. \end{aligned}$$

Since

$$\frac{1}{\epsilon} - \frac{c}{2} > 0 \quad \text{and} \quad 1 - \beta - \frac{c}{2} > 0,$$

by assumption, it follows that

$$(F(x), x) \leq \alpha - \delta \|x\|^2,$$

where $\alpha = \beta + 1/\epsilon > 0$ and $\delta = \min\{1/\epsilon - c/2, 1 - \beta - c/2\} > 0$. \square

Note that the conditions on the model parameters in Proposition 6.1 are satisfied, e.g., if $\gamma = 1/\epsilon$ and $\beta < 1$. Such parameter settings may be relevant in applications, see Section 7.

6.1 Splitting methods for the FHN model

The FHN model (40) is a semi-linear SDE of type (1). The choice of the matrix A and the function $N(X(t))$ is not unique. While the locally Lipschitz term $-V^3(t)/\epsilon$ and the constant β have to enter into $N(X(t))$, the goal is to allocate the remaining terms such that as many of the introduced assumptions as possible are satisfied. For the splitting methods to be 1-step hypoelliptic, the term $-U(t)/\epsilon$ of the first component of the drift must enter into $AX(t)$. Moreover, shifting the term $\gamma V(t)$ to $AX(t)$ leads to a decoupling of the resulting ODE (13) such that its global solution can be derived explicitly, guaranteeing Assumption (A3). Thus, there are four strategies left, depending on whether the remaining terms $V(t)/\epsilon$ and $-U(t)$ enter into $AX(t)$ or $N(X(t))$. The only case where the matrix A meets Assumption (A5) (under a restricted parameter space) is when $-U(t)$ appears in $AX(t)$ and $V(t)/\epsilon$ in $N(X(t))$. Similar to the proposed splitting of SDE (37), the resulting linear SDE (12) is then geometrically ergodic. In particular, it corresponds to a version of the well-studied damped stochastic harmonic oscillator whose matrix exponential e^{At} and covariance matrix $C(t)$ have manageable expressions. Therefore, we propose to choose the matrix A and the function N as follows

$$A = \begin{pmatrix} 0 & -\frac{1}{\epsilon} \\ \gamma & -1 \end{pmatrix}, \quad N(X(t)) = \begin{pmatrix} \frac{1}{\epsilon}(V(t) - V^3(t)) \\ \beta \end{pmatrix}. \quad (42)$$

The resulting linear damped stochastic harmonic oscillator (12) with A as in (42) is weakly-, critically- or over-damped, depending on whether

$$\kappa := \frac{4\gamma}{\epsilon} - 1 \quad (43)$$

is positive, zero or negative, respectively [10, 37, 52]. In particular, the sign of κ determines the shape of the exponential of the matrix A . If $\kappa = 0$,

$$e^{At} = e^{-\frac{t}{2}} \begin{pmatrix} 1 + \frac{t}{2} & -\frac{t}{\epsilon} \\ \frac{\epsilon t}{4} & 1 - \frac{t}{2} \end{pmatrix}.$$

If $\kappa > 0$,

$$e^{At} = e^{-\frac{t}{2}} \begin{pmatrix} \cos(\frac{1}{2}\sqrt{\kappa}t) + \frac{1}{\sqrt{\kappa}} \sin(\frac{1}{2}\sqrt{\kappa}t) & -\frac{2}{\epsilon\sqrt{\kappa}} \sin(\frac{1}{2}\sqrt{\kappa}t) \\ \frac{2\gamma}{\sqrt{\kappa}} \sin(\frac{1}{2}\sqrt{\kappa}t) & \cos(\frac{1}{2}\sqrt{\kappa}t) - \frac{1}{\sqrt{\kappa}} \sin(\frac{1}{2}\sqrt{\kappa}t) \end{pmatrix}.$$

If $\kappa < 0$, the sine and cosine terms of the above expressions can be rearranged using the relations

$$\cos\left(\frac{1}{2}\sqrt{\kappa}t\right) = \cosh\left(\frac{1}{2}\sqrt{-\kappa}t\right) \quad \text{and} \quad \frac{1}{\sqrt{\kappa}} \sin\left(\frac{1}{2}\sqrt{\kappa}t\right) = \frac{1}{\sqrt{-\kappa}} \sinh\left(\frac{1}{2}\sqrt{-\kappa}t\right). \quad (44)$$

Moreover, the covariance matrix $C(t)$ (15) also depends on the sign of κ and is given as follows. If $\kappa = 0$,

$$\begin{aligned} c_{11}(t) &= \frac{e^{-t}}{4\epsilon^2} (4\sigma_2^2 (-2 + 2e^t - t(2+t)) + \epsilon^2 \sigma_1^2 (-10 + 10e^t - t(6+t))), \\ c_{12}(t) &= c_{21}(t) = \frac{e^{-t}}{8\epsilon} (-4\sigma_2^2 t^2 + \epsilon^2 \sigma_1^2 (4e^t - (2+t)^2)), \\ c_{22}(t) &= \frac{e^{-t}}{16} (4\sigma_2^2 (-2 + 2e^t - (t-2)t) + \epsilon^2 \sigma_1^2 (-2 + 2e^t - t(2+t))). \end{aligned}$$

If $\kappa > 0$,

$$\begin{aligned} c_{11}(t) &= \frac{\epsilon e^{-t}}{2\gamma\kappa} \left(-\frac{4\gamma}{\epsilon^2} (\sigma_1^2 \gamma + \sigma_2^2 \frac{1}{\epsilon}) + \kappa e^t (\sigma_1^2 (1 + \frac{\gamma}{\epsilon}) + \sigma_2^2 \frac{1}{\epsilon^2}) \right. \\ &\quad \left. + \left(\sigma_1^2 (1 - \frac{3\gamma}{\epsilon}) + \sigma_2^2 \frac{1}{\epsilon^2} \right) \cos(\sqrt{\kappa}t) - \sqrt{\kappa} (\sigma_1^2 (1 - \frac{\gamma}{\epsilon}) + \sigma_2^2 \frac{1}{\epsilon^2}) \sin(\sqrt{\kappa}t) \right), \\ c_{12}(t) &= c_{21}(t) = \frac{\epsilon e^{-t}}{2\kappa} \left(\sigma_1^2 \kappa e^t - \frac{2}{\epsilon} (\sigma_1^2 \gamma + \sigma_2^2 \frac{1}{\epsilon}) \right. \\ &\quad \left. + \left(\sigma_1^2 (1 - \frac{2\gamma}{\epsilon}) + 2\sigma_2^2 \frac{1}{\epsilon^2} \right) \cos(\sqrt{\kappa}t) - \sigma_1^2 \sqrt{\kappa} \sin(\sqrt{\kappa}t) \right), \\ c_{22}(t) &= \frac{\epsilon e^{-t}}{2\kappa} \left((\sigma_2^2 \frac{1}{\epsilon} + \sigma_1^2 \gamma) \left(\cos(\sqrt{\kappa}t) - \frac{4\gamma}{\epsilon} + \kappa e^t \right) + (\sigma_2^2 \frac{1}{\epsilon} - \sigma_1^2 \gamma) \sqrt{\kappa} \sin(\sqrt{\kappa}t) \right). \end{aligned}$$

If $\kappa < 0$, the relations (44) can again be used to rewrite the above expressions accordingly. Note that parameter configurations typically considered in the literature fulfill $\kappa > 0$, see, e.g., [17, 36, 13]. This is in agreement with the fact that, under $\kappa > 0$, SDE (12) models a weakly damped system which describes oscillatory dynamics.

The locally Lipschitz function N in (42) satisfies Assumptions (A1) and (A2).

Proposition 6.2. *Let $N : \mathbb{R}^2 \rightarrow \mathbb{R}^2$ be as in (42). Then N satisfies Assumptions (A1) and (A2).*

Proof. The proof is given in Appendix C. \square

Moreover, the explicit solution of ODE (13) with $N(X(t))$ as in (42) is given by

$$X^{[2]}(t) = f(X_0^{[2]}; t) = \begin{pmatrix} \frac{V_0^{[2]}}{\sqrt{e^{-\frac{2t}{\epsilon}} + (V_0^{[2]})^2 (1 - e^{-\frac{2t}{\epsilon}})}} \\ \beta t + U_0^{[2]} \end{pmatrix}, \quad (45)$$

and thus Assumption (A3) is satisfied.

The well-defined Lie-Trotter and Strang splitting methods for the FHN model (40) are then given by (18) and (19), respectively, where the matrix exponential $e^{A\Delta}$, the covariance matrix $C(\Delta)$ and the function f are as reported above.

6.2 Mean-square convergence

In the following proposition, we verify Assumptions (A4.1) and (A4.2) (under $\beta = 0$), which are required to establish the mean-square boundedness of the splitting methods under Part I and Part II of Lemma 4.2, respectively.

Proposition 6.3. *Let $f : \mathbb{R}^2 \rightarrow \mathbb{R}^2$ be as in (45).*

Part I: Then f satisfies Assumption (A4.1).

Part II: If $\beta = 0$, then f satisfies Assumption (A4.2).

Proof. The proof is given in Appendix D. □

Thus, using Theorem 4.2, the Lie-Trotter (18) and Strang (19) splitting methods applied to the FHN model are mean-square convergent of order 1. While for the Lie-Trotter splitting this result holds without any restrictions on the parameter space of the model, we require $\beta = 0$ for the Strang method. However, since compositions based on fractional steps usually improve the performance of a splitting method rather than deteriorating it, it is expected that the Strang method is also mean-square convergent for any $\beta \geq 0$. This is confirmed in our experiments.

6.3 Structure preservation

1-step hypoellipticity Recall that, if $\sigma_1 = 0$, the FHN model (40) is hypoelliptic. Due to the choice of the matrix A as in (42), the linear stochastic subequation (12) of the splitting framework is also hypoelliptic. In particular, Condition (5), which is given by

$$\partial_u(Ax)_1\sigma_2 = -\frac{\sigma_2}{\epsilon} \neq 0,$$

and coincides with (41) for the FHN model, holds. Therefore, the splitting methods (18) and (19) are 1-step hypoelliptic and the Lie-Trotter splitting (18) yields a non-degenerate conditional Gaussian distribution according to Theorem 5.1. In particular, its conditional covariance matrix coincides with $C(\Delta)$ reported above, which is of full rank even if $\sigma_1 = 0$, independently of the value of κ . Moreover, the diagonal terms of $C(\Delta)$ are of the same order with respect to Δ , which is also relevant for likelihood-based inference tools, see, e.g., [17]. Note that, as for the mean-square convergence of the Lie-Trotter method, these results hold without any restrictions on the parameter space.

Geometric ergodicity In the following, we establish the geometric ergodicity of the splitting methods applied to the FHN model under a restricted parameter space. In particular, we require $\beta = 0$ and $\gamma = 1/\epsilon$. Recall the validity of Assumption (A4.2) (under $\beta = 0$) from Proposition 6.3. Moreover, we verify Assumption (A5) (under $\gamma = 1/\epsilon$) in the following proposition.

Proposition 6.4. *Let $\gamma = 1/\epsilon$ and $A \in \mathbb{R}^{2 \times 2}$ be as in (42). Then, A satisfies Assumption (A5).*

Proof. The proof is given in Appendix E. □

Note that, under $\gamma = 1/\epsilon$, the logarithmic norm $\mu(A) = 0$. Thus, Assumption (A6) is not fulfilled and the asymptotic bounds of Corollary 5.1 cannot be derived. However, since Assumptions (A4.2) and (A5) hold under $\beta = 0$ and $\gamma = 1/\epsilon$, respectively, and, under these parameter restrictions, $L(x) = 1 + \|x\|^2$ is a Lyapunov function for the FHN model (40) according to Proposition 6.1, the splitting methods (18) and (19) satisfy the discrete Lyapunov condition of Definition 5.2. This is a direct consequence of Theorem 5.2. Combined with the 1-step hypoellipticity and a discrete irreducibility condition, which can be proved in the same way as done, e.g., in [2, 12, 40], the splitting methods applied to the FHN model are geometrically ergodic. Intuitively, the Lyapunov

structure of the FHN model is kept by the numerical solutions, since the linear SDE (12) determined by the matrix A in (42) is geometrically ergodic, implying that the process $(X^{[1]}(t))_{t \in [0, T]}$ converges to a unique invariant distribution given by

$$X^{[1]}(t) \xrightarrow[t \rightarrow \infty]{\mathcal{D}} \mathcal{N} \left(\begin{pmatrix} 0 \\ 0 \end{pmatrix}, \begin{pmatrix} \frac{5}{2}\sigma_1^2 + \frac{2}{\epsilon^2}\sigma_2^2 & \frac{\epsilon}{2}\sigma_1^2 \\ \frac{\epsilon}{2}\sigma_1^2 & \frac{\epsilon^2}{8}\sigma_1^2 + \frac{1}{2}\sigma_2^2 \end{pmatrix} \right),$$

for $\kappa = 0$, and

$$X^{[1]}(t) \xrightarrow[t \rightarrow \infty]{\mathcal{D}} \mathcal{N} \left(\begin{pmatrix} 0 \\ 0 \end{pmatrix}, \begin{pmatrix} \frac{\epsilon}{2\gamma}(\sigma_1^2 + \frac{\gamma}{\epsilon}\sigma_1^2 + \frac{1}{\epsilon^2}\sigma_2^2) & \frac{\epsilon}{2}\sigma_1^2 \\ \frac{\epsilon}{2}\sigma_1^2 & \frac{1}{2}(\epsilon\gamma\sigma_1^2 + \sigma_2^2) \end{pmatrix} \right),$$

for $\kappa > 0$. Since this fact holds without any restrictions of the parameters, it is expected that the splitting methods preserve this property for any values of $\gamma > 0$ and $\epsilon > 0$. This is confirmed in our experiments.

Remark 6.1. *Another plausible choice of the subequations is*

$$A = \begin{pmatrix} 0 & -\frac{1}{\epsilon} \\ \gamma & 0 \end{pmatrix}, \quad N(X(t)) = \begin{pmatrix} \frac{1}{\epsilon}(V(t) - V^3(t)) \\ -U(t) + \beta \end{pmatrix}.$$

For this choice, Assumptions (A1)-(A4.1) related to the locally Lipschitz function N are satisfied. Moreover, Assumption (A4.2) also holds under $\beta = 0$. Thus, the splitting methods are mean-square convergent. In addition, since the term $-U(t)/\epsilon$ still enters into $AX(t)$, they are also 1-step hypoelliptic. However, in this case, the linear SDE (12) corresponds to a version of the simple (undamped) harmonic oscillator which is not ergodic. In particular, its matrix exponential is given by

$$e^{At} = \begin{pmatrix} \cos(\frac{\sqrt{\gamma}t}{\sqrt{\epsilon}}) & -\frac{1}{\sqrt{\epsilon\gamma}}\sin(\frac{\sqrt{\gamma}t}{\sqrt{\epsilon}}) \\ \sqrt{\epsilon\gamma}\sin(\frac{\sqrt{\gamma}t}{\sqrt{\epsilon}}) & \cos(\frac{\sqrt{\gamma}t}{\sqrt{\epsilon}}) \end{pmatrix},$$

with $\|e^{A\Delta}\| \geq 1$ and $\|e^{A\Delta}\| = 1$ under $\gamma = 1/\epsilon$.

7 Numerical experiments for the FHN model

We now illustrate the performance of the proposed splitting methods in comparison with Euler-Maruyama type methods through a variety of numerical experiments carried out on the FHN model (40). First, the proved mean-square convergence order 1 is illustrated numerically. Second, the ability of the different numerical methods to preserve the qualitative dynamics of neuronal spiking is analysed, in particular the correct amplitudes and frequencies of the underlying oscillations when the time step Δ is increased. Third, the robustness of the numerical methods to changes in the initial condition X_0 , and how the choice of X_0 may influence the preservation of the phases of the underlying oscillations are analysed. All simulations are carried out in the computing environment R [55].

7.1 Convergence order

The mean-square convergence order can be illustrated by approximating the left-hand side of the inequality in (2) (for a fixed time T) with the root mean-squared error (RMSE) defined by

$$\text{RMSE}(\Delta) := \left(\frac{1}{M} \sum_{l=1}^M \|X^l(T) - \tilde{X}_\Delta^l(T)\|^2 \right)^{1/2}, \quad (46)$$

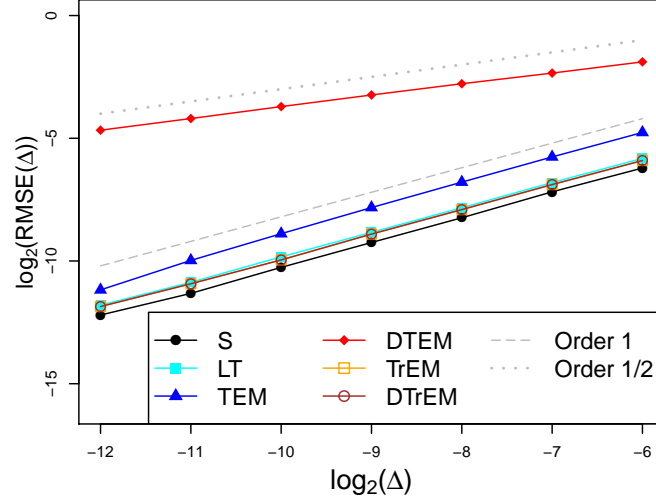


Figure 3: Illustration of the mean-square convergence order on the FHN model (40) via the RMSE (46). All model parameters are set to 1, $X_0 = (0, 0)^\top$ and $T = 10$.

Table 1: RMSE (46) for different values of Δ . All parameters are set to 1, $X_0 = (0, 0)^\top$ and $T = 10$.

Δ	S	LT	TEM	DTEM	TrEM	DTrEM
2^{-6}	0.01348	0.01771	0.03683	0.27024	0.01667	0.01667
2^{-7}	0.00689	0.00895	0.01844	0.19696	0.00845	0.00845
2^{-8}	0.00331	0.0044	0.00906	0.14577	0.00417	0.00417
2^{-9}	0.00165	0.00219	0.00441	0.10613	0.00209	0.00209
2^{-10}	0.00082	0.0011	0.00211	0.07643	0.00101	0.00101
2^{-11}	0.0004	0.00053	0.00099	0.05456	0.000513	0.000513
2^{-12}	0.00021	0.00028	0.00043	0.03926	0.00027	0.00027

where $X^l(T)$ and $\tilde{X}_\Delta^l(T)$ denote the l -th simulated path at a fixed time T of the true process and the approximated process, respectively, for $l = 1, \dots, M$. In Figure 3, we report the RMSEs of the different numerical methods in log2 scale as a function of the time step Δ used to simulate $\tilde{X}_\Delta^l(T)$. Since the true process is not known, the reference values $X^l(T)$ are simulated with the TEM method (21) using the small time step $\Delta = 2^{-14}$. We verified that using a different scheme for the simulation of the reference paths does not affect the results of the experiments. The approximated trajectories $\tilde{X}_\Delta^l(T)$ are generated with the LT (18), S (19), TEM (21), DTEM (22), TrEM (23) and DTrEM (24) method, respectively, under different choices of the time step, namely $\Delta = 2^{-k}$, $k = 6, \dots, 12$. We consider $T = 10$, $M = 10^3$, $X_0 = (0, 0)^\top$ and set all model parameters to 1. The theoretical convergence order 1 of the splitting methods, established in Theorem 4.2, is confirmed numerically. The S splitting yields the smallest RMSEs among all considered numerical methods. The RMSEs of the LT splitting almost coincide with that of the two truncated Euler-Maruyama variants. The RMSEs of the tamed Euler-Maruyama methods are larger than those obtained under the splitting and truncated methods. The DTEM method yields the largest RMSEs, and for that method we only observe a convergence of order 1/2. The latter finding is in agreement with the observations in [30]. All RMSEs are also reported in Table 1. It can be observed that the RMSEs of the LT method lie slightly above those obtained under the truncated methods, which are identical (up to the reported precision).

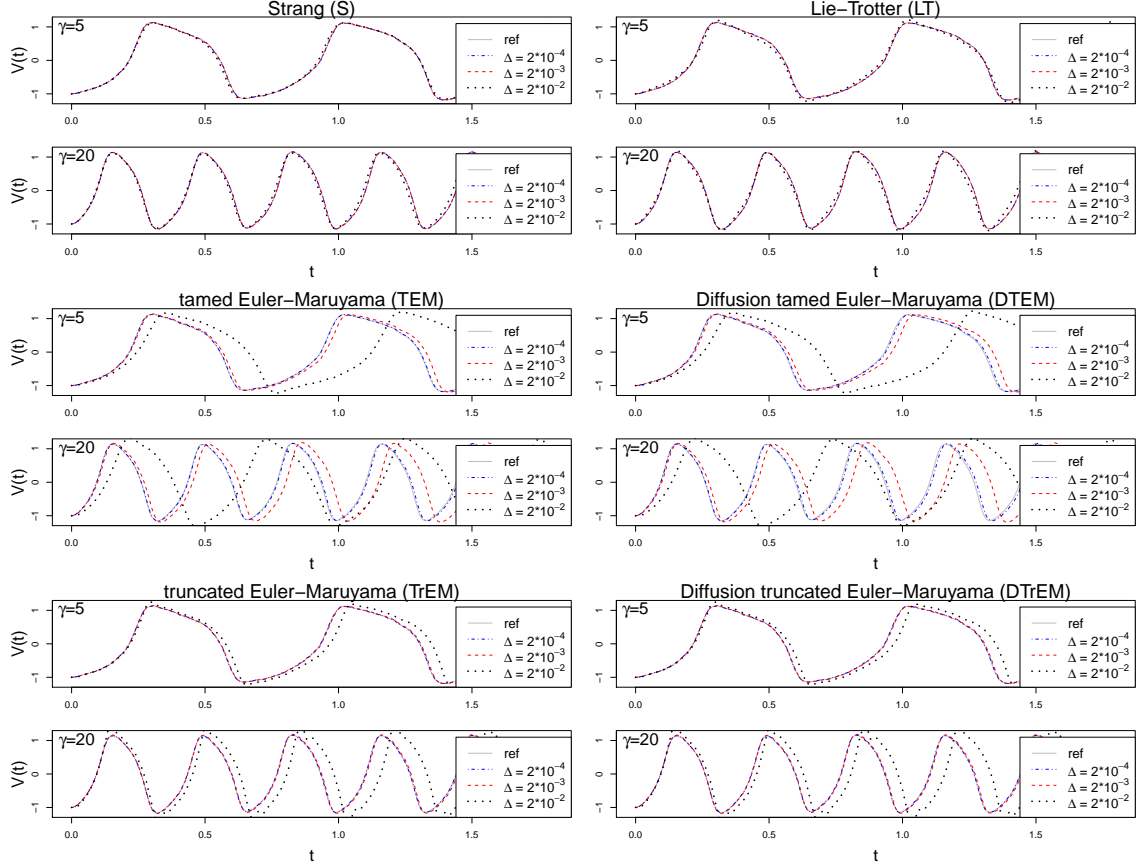


Figure 4: Paths of the V -component of the FHN model (40) simulated under the considered numerical methods for $X_0 = (-1, 0)^\top$, $\beta = \sigma_1 = 0.1$, $\sigma_2 = 0.2$, $\epsilon = 0.05$, two different values of γ and increasing time step Δ .

7.2 Preservation of neuronal spiking dynamics: amplitudes and frequencies

In the following, we analyse the ability of the considered numerical methods to preserve the qualitative neuronal spiking dynamics of the FHN model. In particular, we investigate whether the amplitudes and frequencies of the neuronal oscillations are kept when increasing the time step Δ . Throughout this and the next section, we set $\beta = \sigma_1 = 0.1$ and $\sigma_2 = 0.2$, and consider different values for γ and ϵ . These two parameters are of particular interest, because they regulate the spiking intensity of the neuron and separate the time scale of the two model components, respectively. When ϵ is small, both variables evolve on different time scales. This situation is often referred to as “stiff” case, while larger values of ϵ refer to the “nonstiff” case, see, e.g., [11]. Moreover, these parameters determine the value of $\|e^{A\Delta}\|$, and thus the validity of Theorem 5.2. Since the true process is not available, all reference paths are obtained under the TEM method (21), using the small time step $\Delta = 2 \cdot 10^{-5}$. Also in this case, the choice of the scheme used to simulate the reference paths does not affect the results of the experiments. In the following, the focus lies on the V -component of the equation, modelling the membrane voltage, which can be experimentally recorded with intracellular measurements. Similar results are obtained for the U -component.

In Figure 4, we report paths of the V -component of the FHN model generated under different values of the time step Δ , but using the same underlying pseudo random numbers. An increase in γ leads to an increase in the frequency of the oscillations, and thus in the number of released spikes. Both splitting methods yield almost overlapping paths as Δ increases, preserving thus the qualitative dynamics of the model, independently of the choice of the intensity parameter γ .

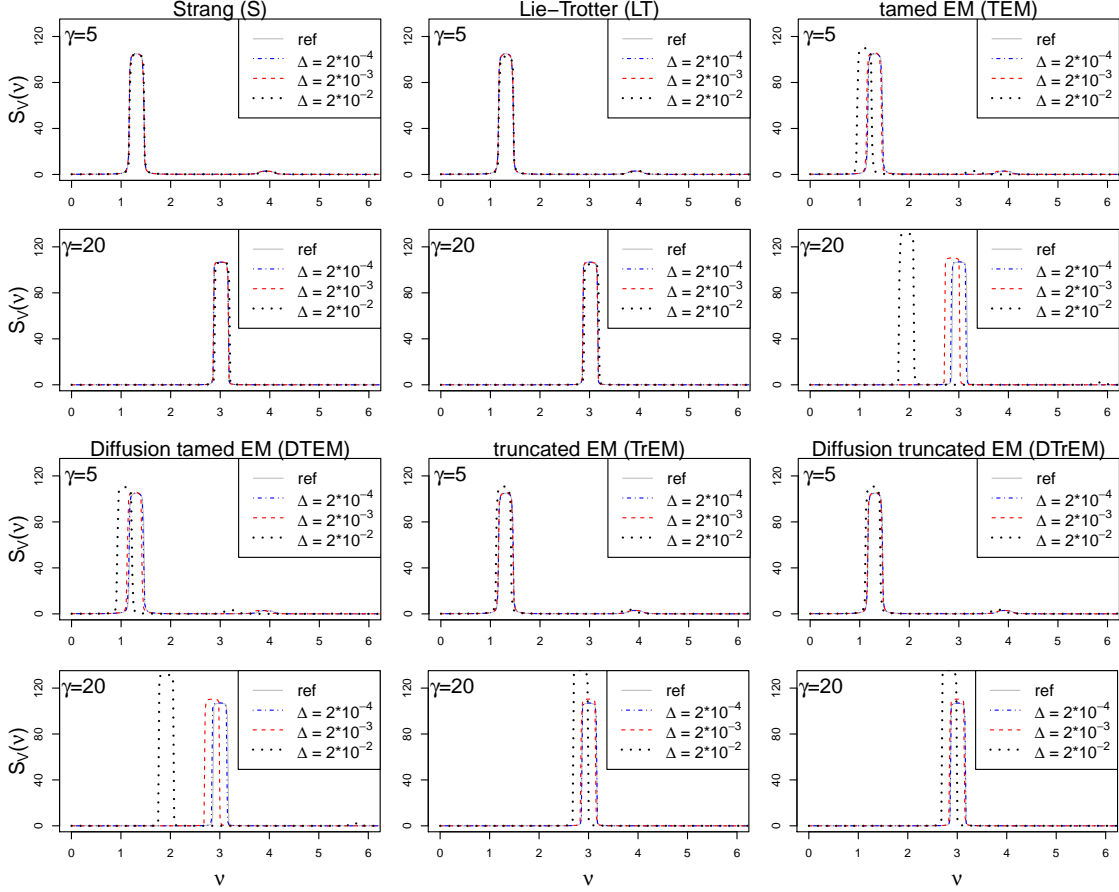


Figure 5: Estimates of the spectral density (47) of the V -component of the FHN model (40) obtained under the considered numerical methods for $X_0 = (0, 0)^\top$, $\beta = \sigma_1 = 0.1$, $\sigma_2 = 0.2$, $\epsilon = 0.05$, two different values of γ and increasing time step Δ .

In contrast, both tamed Euler-Maruyama methods underestimate the frequency and overestimate the amplitude of the neuronal oscillations as Δ increases, for both values of γ under consideration. For similar observations regarding tamed methods, we refer to [29, 30]. Note also that their paths already start deviating from the reference paths for $\Delta = 2 \cdot 10^{-3}$, performing thus worse than the truncated Euler-Maruyama methods.

For a deeper investigation of the neuronal spiking dynamics, we consider the spectral density of the V -component, which takes into account its autocovariance, and thus the dependence of the membrane voltage on previous epochs. It is given by

$$S_V(\nu) = \mathcal{F}\{r_V\}(\nu) = \int_{-\infty}^{\infty} r_V(\tau) e^{-i2\pi\nu\tau} d\tau, \quad (47)$$

where \mathcal{F} denotes the Fourier transformation, r_V the autocovariance function of the stochastic process $(V(t))_{t \in [0, T]}$ and the frequency ν can be interpreted as the number of oscillations in one time unit. We estimate the spectral density $S_V(\nu)$ with a smoothed periodogram estimator, see, e.g., [10, 54], based on paths generated over the time interval $[0, 10^3]$. We use the R-function `spectrum` and set the required smoothing parameter to `span = 0.3T`.

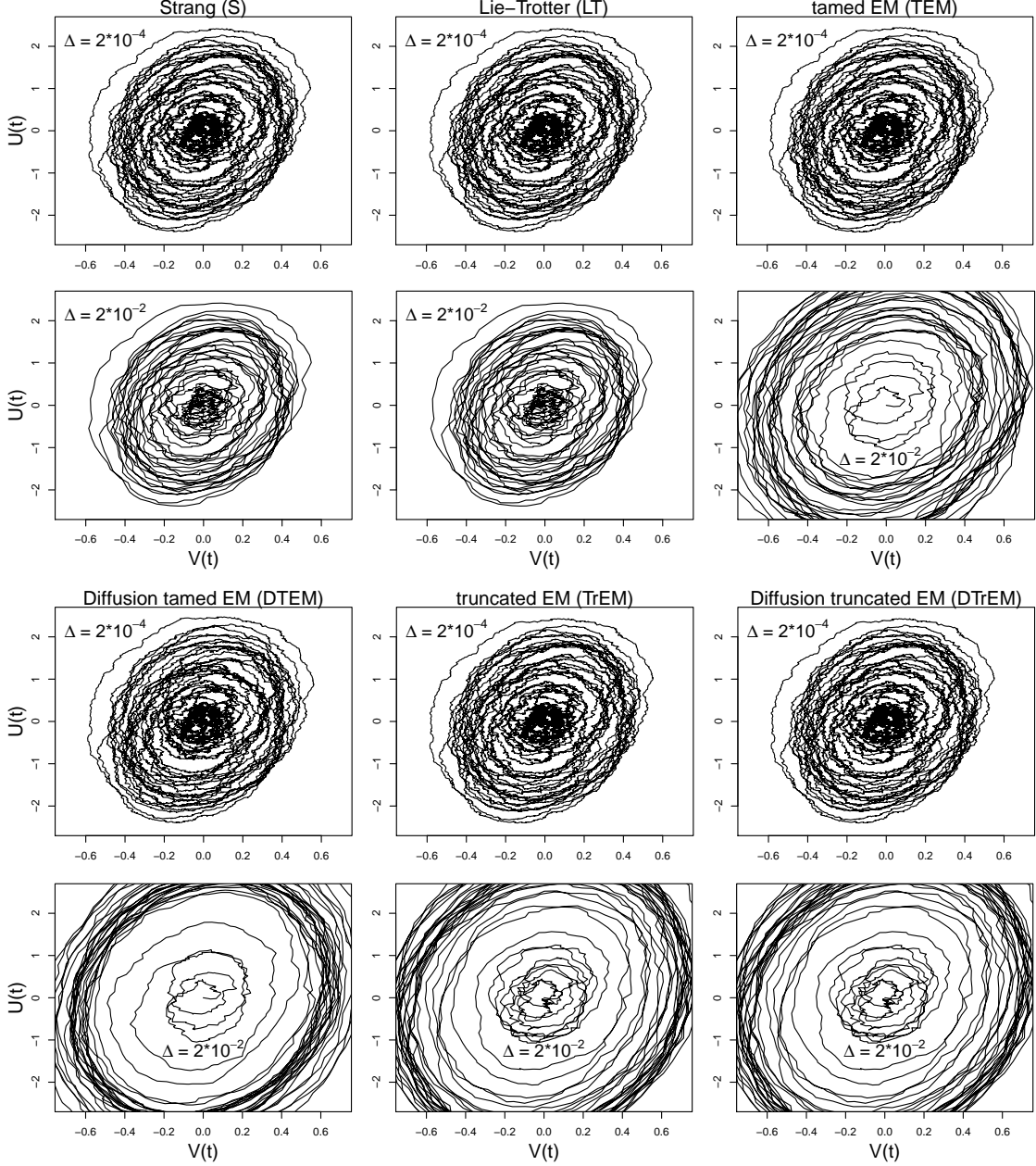


Figure 6: Phase portraits of the FHN model (40) simulated under the considered numerical methods for $X_0 = (0, 0)^\top$, $\beta = \sigma_1 = 0.1$, $\sigma_2 = 0.2$, $\epsilon = 1$, $\gamma = 20$ and increasing time step Δ .

The estimated spectral densities obtained under different values of γ and different choices of the time step Δ are reported in Figure 5. As desired, for a fixed γ , all spectral densities estimated from the paths generated under the splitting schemes are almost overlapping as Δ increases. In contrast, the frequency ν estimated under the Euler-Maruyama type methods decreases as Δ increases, and the height of the peaks, carrying information about the amplitude of the neuronal oscillations, increases with Δ . Their performance deteriorates as γ increases, the truncated methods yielding better results than the tamed methods. Note also that the estimated frequencies are in agreement with those deduced from Figure 4.

Moreover, all Euler-Maruyama type methods perform even worse in terms of second moment (amplitude) preservation when the parameter ϵ is increased, while the splitting methods preserve

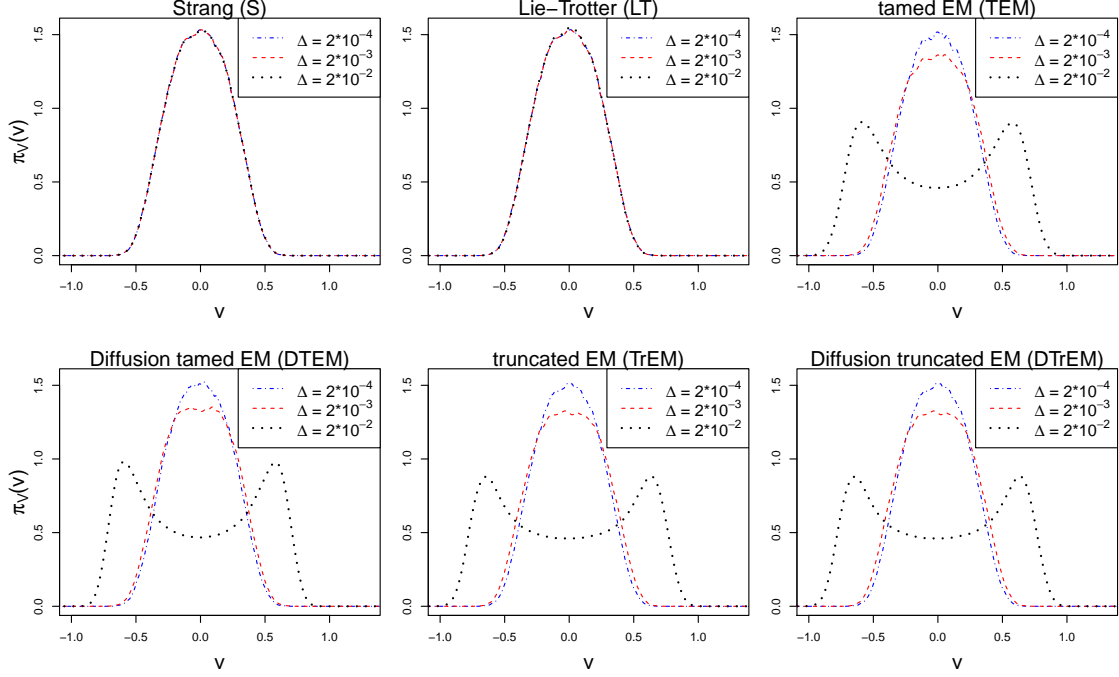


Figure 7: Estimates of the invariant density (48) of the V -component of the FHN model (40) obtained under the considered numerical methods for $X_0 = (0, 0)^\top$, $\beta = \sigma_1 = 0.1$, $\sigma_2 = 0.2$, $\epsilon = 1$, $\gamma = 20$ and increasing time step Δ .

the qualitative behaviour of the model. This is illustrated in Figure 6, where we increase ϵ to 1, fix $\gamma = 20$ and report phase portraits of the system obtained under the different numerical methods for $\Delta = 2 \cdot 10^{-4}$ and $\Delta = 2 \cdot 10^{-2}$. Again, the splitting methods preserve the behaviour of the process $(X(t))_{t \in [0, T]}$ as Δ increases, while the Euler-Maruyama type methods produce larger orbits, overshooting the second moment of the process.

In addition, we investigate the ability of the considered numerical methods to preserve the underlying invariant density of the process $(X(t))_{t \in [0, T]}$. In particular, we estimate the marginal invariant density of the V -component with a standard kernel density estimator given by

$$\pi_V(v) = \frac{1}{nh} \sum_{i=1}^n \mathcal{K} \left(\frac{v - \tilde{V}(t_i)}{h} \right), \quad (48)$$

where h denotes a smoothing bandwidth and \mathcal{K} is a kernel function [53]. Taking advantage of the ergodicity of the FHN model, the sample $\tilde{V}(t_i)$, $i = 1, \dots, n$, in (48) is obtained from a long-time simulation of a single path. We use the R-function `density`, a kernel estimator as in (48).

In Figure 7, we report the marginal invariant densities of the process $(V(t))_{t \in [0, T]}$ estimated via (48) based on paths generated over the time interval $[0, 10^4]$, for $\epsilon = 1$, $\gamma = 20$ and different values of Δ . Both splitting methods yield reliable estimates for all values of Δ under consideration. In contrast, the densities obtained under the Euler-Maruyama type methods already deviate from the desired ones for $\Delta = 2 \cdot 10^{-3}$, and suggest a transition from a unimodal to a bimodal density when Δ is further increased to $2 \cdot 10^{-2}$. It is again visible that the Euler-Maruyama type methods overestimate the second moment, and thus the amplitudes of the process. Similar results are also obtained for the U -component.

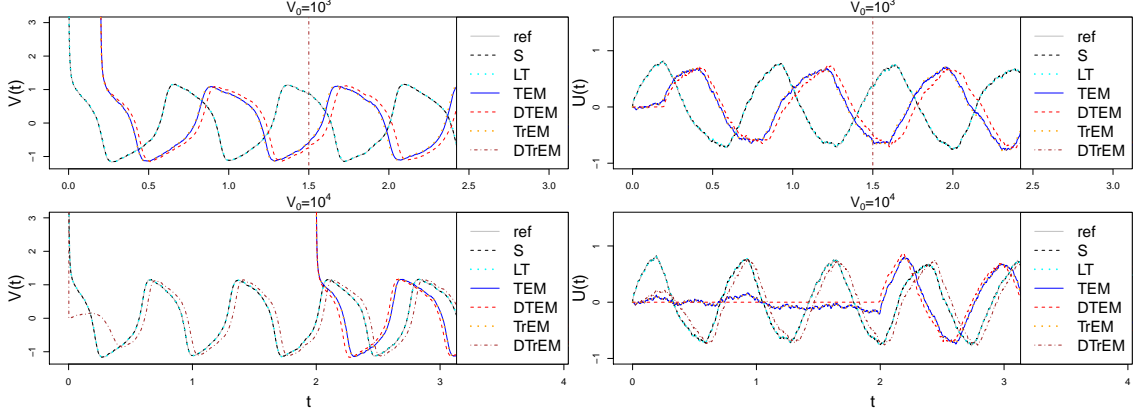


Figure 8: Paths of the V - and U -components of the FHN model (40) simulated under the considered numerical methods for large values of V_0 ($U_0 = 0$), $\Delta = 2 \cdot 10^{-4}$, $\beta = \sigma_1 = 0.1$, $\sigma_2 = 0.2$, $\gamma = 5$ and $\epsilon = 0.05$. The grey reference paths are obtained under $\Delta = 2 \cdot 10^{-7}$ using the TEM method (21).

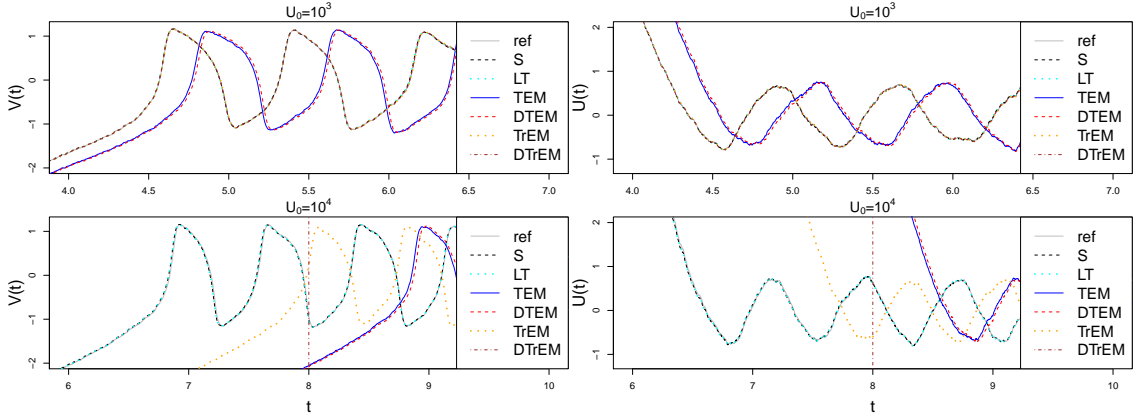


Figure 9: Paths of the V - and U -components of the FHN model (40) simulated under the considered numerical methods for large values of U_0 ($V_0 = 0$), $\Delta = 2 \cdot 10^{-4}$, $\beta = \sigma_1 = 0.1$, $\sigma_2 = 0.2$, $\gamma = 5$ and $\epsilon = 0.05$. The grey reference paths are obtained under $\Delta = 2 \cdot 10^{-7}$ using the TEM method (21).

7.3 Impact of the initial condition: preservation of phases

Finally, we compare the considered numerical methods regarding their sensitivity to changes in X_0 , as done in Section 5.2 for SDE (37). In particular, we illustrate that, when V_0 or U_0 are large, the considered Euler-Maruyama type methods do not correctly reproduce the phases of the underlying oscillations, even when the time step Δ is very small. In contrast, the splitting methods are less sensitive to changes in the starting condition.

The impact of V_0 is shown in Figure 8, where we report paths of the V -component (left panels) and the U -component (right panels), simulated under the different numerical methods with $\Delta = 2 \cdot 10^{-4}$, $U_0 = 0$, $V_0 = 10^3$ (top panels) and $V_0 = 10^4$ (bottom panels). The grey reference path is simulated under $\Delta = 2 \cdot 10^{-7}$ using the TEM method (21). As before, the results are not influenced by the choice of the numerical method used to generate the reference paths. The underlying parameter values are the same as in Section 7.2, setting $\gamma = 5$ and $\epsilon = 0.05$. As desired, the splitting methods are barely influenced by V_0 , even when it is very large, with paths overlapping with the reference paths for all t under consideration. The main reason for this preservative behaviour lies in the exact treatment of the locally Lipschitz ODE via (45). In particular, for the considered values $\epsilon = 0.05$ and $\Delta = 2 \cdot 10^{-4}$ we obtain $V^{[2]}(t_1) \approx 11.2$

already after the first iteration for both $V_0 = 10^3$ and $V_0 = 10^4$. In contrast, the Euler-Maruyama type methods introduce a delay in when the generated paths reach the oscillatory dynamics, this behaviour deteriorating as V_0 increases. Moreover, they also do not preserve the phases of the oscillations, introducing a shift. The DTrEM method reaches the correct oscillatory dynamics, though shifted, almost as fast as the splitting methods for $V_0 = 10^4$, but fails for $V_0 = 10^3$. This is indicated by the brown vertical lines in the top panels of Figure 8. In that case, this method produces almost constant values $\tilde{V}(t_i) \approx 10^3$, and thus does not enter the oscillatory regime. Spurious oscillations were obtained for other parameter combinations, as also observed in [30, 62].

Similar observations can be drawn from Figure 9, where we set $V_0 = 0$ and consider $U_0 = 10^3$ (top panels) and $U_0 = 10^4$ (bottom panels). From the top panels of Figure 9, it can be observed that the truncated Euler-Maruyama methods preserve the initial behaviour of the process for $U_0 = 10^3$. However, they both fail when $U_0 = 10^4$, with the TrEM method (23) yielding shifted trajectories and the DTrEM method (24) not entering into the oscillatory regime. The latter fact is indicated by the brown vertical lines in the bottom panels of Figure 9. The tamed Euler-Maruyama methods lead to shifted paths in both considered scenarios. In contrast, the splitting methods overlap with the grey reference paths of the U -component for all t under consideration, preserving the phases of the oscillations.

Remark 7.1. *Note that the only considered combination of γ and ϵ in this section for which Assumption (A5), and thus Theorem 5.2 holds is $\gamma = 1/\epsilon = 20$. However, we do not observe a difference in the quality of the splitting methods depending on the combination of these parameters. Intuitively, this is because the underlying linear SDE (12) with matrix A as in (42), i.e., the damped stochastic oscillator, is geometrically ergodic for all $\gamma > 0$ and $\epsilon > 0$.*

8 Conclusion

We construct explicit and reliable numerical splitting methods to approximate the solutions of semi-linear SDEs with additive noise and globally one-sided Lipschitz continuous drift coefficients which are allowed to grow polynomially at infinity. We prove that the derived splitting methods are mean-square convergent of order 1, under an assumption on the explicit solution of the deterministic subequation containing the locally Lipschitz drift term. In particular, two versions for the proof of the boundedness of the second moment of the splitting methods, each requiring a different assumption, are provided. In contrast to existing explicit mean-square convergent Euler-Maruyama type methods, which may also achieve a convergence rate of order 1, the proposed splitting methods preserve important structural properties of the model.

First, they provide a more accurate approximation of the noise structure of the SDE through the covariance matrix of the explicit solution of the stochastic subequation. In particular, while the conditional covariance matrix of Euler-Maruyama type methods only contains the information of the diffusion matrix Σ , the splitting methods also rely on the matrix A in the semi-linear drift. This is particularly beneficial when the SDE is hypoelliptic. While the conditional covariance matrix of the existing methods is degenerate in that case, we establish the 1-step hypoellipticity of the constructed splitting methods, meaning that they admit a smooth transition density in every iteration step. In particular, the Lie-Trotter splitting yields non-degenerate Gaussian transition densities, a feature which is advantageous within likelihood-based estimation techniques, where the existing numerical methods cannot be applied due to the degenerate covariance matrix [17, 42, 52].

Second, Euler-Maruyama type methods do not preserve the geometric ergodicity of the process. As a consequence, they are not robust to changes in the initial condition, yield poor approximations of the underlying invariant distribution, or do not preserve the moments of the process. In contrast, the proposed splitting methods are proved to preserve the Lyapunov structure of the SDE, as long as $\|e^{A\Delta}\| < 1$ for all $\Delta \in (0, \Delta_0]$. In addition, if the logarithmic norm $\mu(A) < 0$, they are proved to have asymptotically bounded second moments. In the one-dimensional case, closed-form expressions for the precise bounds of the second moments of the splitting methods are derived and illustrated on a cubic model problem. We also consider the FHN model, a well known equation

used to describe the firing activity of single neurons. The geometric ergodicity of the proposed splitting methods applied to this equation is established under a restricted parameter space.

Third, we illustrate on the FHN model that, in contrast to Euler-Maruyama type methods, the proposed splitting methods preserve the amplitudes, frequencies and phases of neuronal oscillations, even for large time steps. As the considered Euler-Maruyama type methods do converge, their lack of structure preservation becomes less visible when using very small time steps. However, the use of significantly smaller time steps results in drastically higher computational costs, making these methods highly inefficient and, consequently, computationally infeasible within simulation-based inference algorithms, as previously illustrated in [10]. Among all considered methods, the Strang splitting shows the best performance in terms of preserving the qualitative dynamics of neuronal spiking. This makes the method particularly beneficial when used, e.g., to simulate large networks of neurons, or when embedded within simulation-based inference procedures.

Several generalisations of the considered approach are possible. The proposed splitting methods can be, e.g., applied to the stochastic Van der Pol oscillator [65, 66], whose investigation leads to similar numerical results. Moreover, they may be extended to SDEs with multiplicative noise, e.g., to $\Sigma(X(t)) = \sqrt{X(t)}$ or $\Sigma(X(t)) = \sigma X(t)$, $\sigma > 0$, where the stochastic subequation of the splitting framework corresponds to the square-root process (also known as Cox-Ingersoll-Ross model [15]) or to the geometric Brownian motion, respectively. A prominent example for the latter one is the stochastic Ginzburg-Landau equation arising from the theory of superconductivity [19, 26]. Furthermore, the proposed splitting methods may be extended to SDEs with more general functions N , requiring to relax Assumption (A3). In addition, one may extend the range of structural properties which characterise the quality of the considered numerical methods.

References

- [1] M. Ableidinger and E. Buckwar. Splitting integrators for the stochastic Landau–Lifshitz equation. *SIAM J. Sci. Comput.*, 38:A1788–A1806, 2016.
- [2] M. Ableidinger, E. Buckwar, and H. Hinterleitner. A stochastic version of the Jansen and Rit neural mass model: analysis and numerics. *J. Math. Neurosci.*, 7(8), 2017.
- [3] L. A. Alyushina. Euler polygonal lines for Itô equations with monotone coefficients. *Theory Probab. Its Appl.*, 32(2):340–345, 1988.
- [4] L. Arnold. *Stochastic Differential Equations: Theory and Applications*. Wiley, New York, 1974.
- [5] N. Berglund and D. Landon. Mixed-mode oscillations and interspike interval statistics in the stochastic FitzHugh-Nagumo model. *Nonlinearity*, 25(8):2303–2335, 2012.
- [6] S. Blanes, F. Casas, and A. Murua. Splitting and composition methods in the numerical integration of differential equations. *Bol. Soc. Esp. Mat. Apl.*, 45, 2009.
- [7] S. Bonaccorsi and E. Mastrogiacomo. Analysis of the stochastic FitzHugh-Nagumo system. *Infin. Dimens. Anal. Quantum Probab. Relat. Top.*, 11(03):427–446, 2008.
- [8] N. Bou-Rabee. Cayley splitting for second-order Langevin stochastic partial differential equations. <https://arxiv.org/abs/1707.05603>, 2017.
- [9] C. E. Bréhier and L. Goudenège. Analysis of some splitting schemes for the stochastic Allen-Cahn equation. *Discrete Cont. Dyn.-B*, 24:4169–4190, 2019.
- [10] E. Buckwar, M. Tamborrino, and I. Tubikanec. Spectral density-based and measure-preserving ABC for partially observed diffusion processes. An illustration on Hamiltonian SDEs. *Stat. Comput.*, 30(3):627–648, 2020.

- [11] Z. Chen, B. Raman, and A. Stern. Structure-preserving numerical integrators for Hodgkin–Huxley-type systems. *SIAM J. Sci. Comput.*, 42(1):B273–B298, 2020.
- [12] J. Chevallier, A. Melnykova, and I. Tubikanec. Theoretical analysis and simulation methods for Hawkes processes and their diffusion approximation. *Oberwolfach Preprints (MFO)* <https://doi.org/10.14760/OWP-2020-09>, 2020.
- [13] Q. Clairon and A. Samson. Optimal control for estimation in partially observed elliptic and hypoelliptic linear stochastic differential equations. *Stat. Inference Stoch. Process.*, 23(1):105–127, 2020.
- [14] D. Cohen. On the numerical discretisation of stochastic oscillators. *Math. Comput. Simul.*, 82(8):1478–1495, 2012.
- [15] J.C. Cox, J. Ingersoll, and S. Ross. A theory of the term structure of interest rates. *Econometrica*, 53(02):385–407, 1985.
- [16] G. Da Prato and J. Zabczyk. *Ergodicity for infinite dimensional systems*. London Mathematical Society Lecture Note Series. Cambridge University Press, 1996.
- [17] S. Ditlevsen and A. Samson. Hypoelliptic diffusions: filtering and inference from complete and partial observations. *J. Royal Stat. Soc. B*, 81(2):361–384, 2019.
- [18] R. FitzHugh. Impulses and physiological states in theoretical models of nerve membrane. *Biophys. J.*, 1(6):445–466, 1961.
- [19] V. L. Ginzburg and L. D. Landau. On the theory of superconductivity. *Zh. Eksp. Teor. Fiz.*, 20:1064–1082, 1950.
- [20] E. Hairer, C. Lubich, and G. Wanner. *Geometric Numerical Integration*. Springer, Heidelberg, 2006.
- [21] E. Hairer, S. P. Nørsett, and G. Wanner. *Solving Ordinary Differential Equations: Nonstiff Problems*. Springer, Berlin, second edition, 2000.
- [22] D. J. Higham, X. Mao, and A. M. Stuart. Strong convergence of Euler-type methods for nonlinear stochastic differential equations. *SIAM J. Numer. Anal.*, 40:1041–1063, 2002.
- [23] A. L. Hodgkin and A. F. Huxley. A quantitative description of membrane current and its application to conduction and excitation in nerve. *J. Physiol.*, 117(4):500–544, 1952.
- [24] A. R. Humphries and A. M. Stuart. *Deterministic and random dynamical systems: Theory and numerics*. In: Bourlioux A., Gander M. J., Sabidussi G. (eds) *Modern Methods in Scientific Computing and Applications. NATO Science Series (Series II: Mathematics, Physics and Chemistry)*, vol 75., pages 211–254. Springer Netherlands, Dordrecht, 2002.
- [25] M. Hutzenthaler and A. Jentzen. Numerical approximations of stochastic differential equations with non-globally Lipschitz continuous coefficients. *Mem. Am. Math. Soc.*, 236, 2012.
- [26] M. Hutzenthaler, A. Jentzen, and P. E. Kloeden. Strong and weak divergence in finite time of Euler’s method for stochastic differential equations with non-globally Lipschitz continuous coefficients. *Proc. R. Soc. A*, 467:1563–1576, 2011.
- [27] M. Hutzenthaler, A. Jentzen, and P. E. Kloeden. Strong convergence of an explicit numerical method for SDEs with nonglobally Lipschitz continuous coefficients. *Ann. Appl. Probab.*, 22(4):1611–1641, 2012.
- [28] M. Hutzenthaler and A. Wakolbinger. Ergodic behavior of locally regulated branching populations. *Ann. Appl. Probab.*, 17(20):474–501, 2007.

- [29] C. Kelly and G. Lord. Adaptive time-stepping strategies for nonlinear stochastic systems. *Ima. J. Numer. Anal.*, 38(3):1523–1549, 2017.
- [30] C. Kelly and G. Lord. Adaptive Euler methods for stochastic systems with non-globally Lipschitz coefficients. <https://arxiv.org/abs/1805.11137>, 2018.
- [31] R. Khasminskii. *Stochastic Stability of Differential Equations*. Springer, second edition, 2011.
- [32] R. Khasminskii and F. C. Klebaner. Long term behavior of solutions of the Lotka-Volterra system under small random perturbations. *Ann. Appl. Probab.*, 11(3):952–963, 2001.
- [33] P. E. Kloeden and E. Platen. *Numerical Solution of Stochastic Differential Equations*. Springer, Berlin, 1992.
- [34] N. V. Krylov. A simple proof of the existence of a solution of Itô’s equation with monotone coefficients. *Theory Probab. Its Appl.*, 35(3):583–587, 1991.
- [35] B. Leimkuhler and C. Matthews. *Molecular Dynamics: With Deterministic and Stochastic Numerical Methods*. Springer International Publ., Cham, 2015.
- [36] J.R. León and A. Samson. Hypocoelliptic stochastic FitzHugh-Nagumo neuronal model: mixing, up-crossing and estimation of the spike rate. *Ann. Appl. Probab.*, 28(4):2243–2274, 2018.
- [37] X. Mao. *Stochastic Differential Equations and Applications*. Horwood Publications, Chichester, 1997.
- [38] X. Mao. The truncated Euler–Maruyama method for stochastic differential equations. *J. Comput. Appl. Math.*, 290:370–384, 2015.
- [39] X. Mao. Convergence rates of the truncated Euler–Maruyama method for stochastic differential equations. *J. Comput. Appl. Math.*, 296:362–375, 2016.
- [40] J. C. Mattingly, A. M. Stuart, and D. J. Higham. Ergodicity for SDEs and approximations: locally Lipschitz vector fields and degenerate noise. *Stoch. Process. Their Appl.*, 101(2):185–232, 2002.
- [41] R. McLachlan and G. Quispel. Splitting methods. *Acta Numer.*, 11:341–434, 2002.
- [42] A. Melnykova. Parametric inference for hypoelliptic ergodic diffusions with full observations. *Stat. Inference Stoch. Process.*, 23:595–635, 2020.
- [43] G. N. Milstein. A theorem on the order of convergence of mean-square approximations of solutions of systems of stochastic differential equations. *Theory Probab. Appl.*, 32(4):738–741, 1988.
- [44] G. N. Milstein and M. V. Tretyakov. Quasi-symplectic methods for Langevin-type equations. *Ima. J. Numer. Anal.*, 23(4):593–626, 2003.
- [45] G. N. Milstein and M. V. Tretyakov. *Stochastic Numerics for Mathematical Physics*. Scientific computation. Springer, Berlin, 2004.
- [46] G. N. Milstein and M. V. Tretyakov. Computing ergodic limits for Langevin equations. *Physica D: Nonlinear Phenomena*, 229(1):81–95, 2007.
- [47] T. Misawa. A Lie algebraic approach to numerical integration of stochastic differential equations. *SIAM J. Sci. Comput.*, 23(3):866–890, 2001.
- [48] C. B. Muratov and E. Vanden-Eijnden. Noise-induced mixed-mode oscillations in a relaxation oscillator near the onset of a limit cycle. *Chaos*, 18(1):015111, 2008.

- [49] J. Nagumo, S. Arimoto, and S. Yoshizawa. An active pulse transmission line simulating nerve axon. *Proc. IRE*, 50(10):2061–2070, 1962.
- [50] D. Nualart. *The Malliavin Calculus and Related Topics*. Probability and its applications. Springer, 1995.
- [51] W. P. Petersen. A general implicit splitting for stabilizing numerical simulations of Itô stochastic differential equations. *SIAM J. Numer. Anal.*, 35(4):1439–1451, 1998.
- [52] Y. Pokern, A. M. Stuart, and P. Wiberg. Parameter estimation for partially observed hypoelliptic diffusions. *J. Royal Stat. Soc. B*, 71(1):49–73, 2009.
- [53] O. Pons. *Functional Estimation for Density, Regression Models and Processes*. World Scientific Publishing, Singapore, 2011.
- [54] B. Quinn, I. Clarkson, and R. McKilliam. On the periodogram estimators of periods from interleaved sparse, noisy timing data. *IEEE Stat. Signal Processing Workshop*, pages 232–235, 2014.
- [55] R Development Core Team. *R: A Language and Environment for Statistical Computing*. R Foundation for Statistical Computing, Vienna, Austria, 2011.
- [56] S. Sabanis. A note on tamed Euler approximations. *Electron. Commun. Probab.*, 18(47):1–10, 2013.
- [57] T. Shardlow. Splitting for dissipative particle dynamics. *SIAM J. Sci. Comput.*, 24(4):1267–1282, 2003.
- [58] G. Söderlind. The logarithmic norm. History and modern theory. *BIT Numerical Mathematics*, 46:631–652, 2006.
- [59] G. Strang. On the construction and comparison of difference schemes. *SIAM J. Numer. Anal.*, 5(3):506–517, 1968.
- [60] T. Ström. On logarithmic norms. *SIAM J. Numer. Anal.*, 12(5):741–753, 1975.
- [61] A. H. Strømmen Melbø and D. J. Higham. Numerical simulation of a linear stochastic oscillator with additive noise. *Appl. Numer. Math.*, 51:89–99, 2004.
- [62] M. V. Tretyakov and Z. Zhang. A fundamental mean-square convergence theorem for SDEs with locally Lipschitz coefficients and its applications. *SIAM J. Numer. Anal.*, 51(6):3135–3162, 2013.
- [63] H. F. Trotter. On the product of semi-groups of operators. *Proc. Am. Math. Soc.*, 10(4):545–551, 1959.
- [64] I. Tubikanec, M. Tamborrino, P. Lansky, and E. Buckwar. Qualitative properties of numerical methods for the inhomogeneous geometric Brownian motion. <https://arxiv.org/abs/2003.10193>, 2020.
- [65] B. Van der Pol. A theory of the amplitude of free and forced triode vibrations. *Radio Review*, 1:701–710, 1920.
- [66] B. Van der Pol. On “relaxation-oscillations”. *London Edinburgh Dublin Phil. Mag. J. Sci.*, 2(11):978–992, 1926.

Appendix

A Proof of Proposition 5.1

Proof. We start with Assumption (A1) and have that

$$\begin{aligned} \left(N(x) - N(y)\right)(x - y) &= (x - y - x^3 + y^3)(x - y) \\ &= \left(1 - (x^2 + xy + y^2)\right)(x - y)^2 \leq (x - y)^2. \end{aligned}$$

Thus, the assumption holds for $c_1 = 1$.

Now, consider Assumption (A2). We have that

$$\begin{aligned} \left(N(x) - N(y)\right)^2 &= \left((x - y) + (y^3 - x^3)\right)^2 \\ &\leq 2(x - y)^2 + 2(y^3 - x^3)^2 \\ &= 2(x - y)^2 + 2(x - y)^2(y^2 + xy + x^2)^2 \\ &\leq 2(x - y)^2 + 16(x - y)^2(x^4 + y^4), \end{aligned}$$

where we used that $xy \leq x^2 + y^2$ and that $(2x^2 + 2y^2)^2 \leq 8(x^4 + y^4)$ in the last inequality. Thus, we obtain that

$$\left(N(x) - N(y)\right)^2 \leq 16(x - y)^2(1 + x^4 + y^4),$$

which proves that the assumption holds for $c_2 = 16$ and $\chi = 3$. \square

B Proof of Proposition 5.2

Proof. Setting $y = x^2$, it has to be shown that

$$f^2(x; t) = g(y; t) := \frac{y}{e^{-2t} + y(1 - e^{-2t})} \leq y + \frac{1}{2}t =: h(y; t).$$

Since $g(y; 0) = h(y; 0) = y$, it suffices to prove that for any $y \in \mathbb{R}_0^+$ it holds that

$$g'(y; t) = -\frac{2e^{2t}(y - 1)y}{(1 + (e^{2t} - 1)y)^2} \leq \frac{1}{2} = h'(y; t) \quad \forall t \geq 0,$$

where $'$ denotes the derivative with respect to t . Consider four cases. First, let $y = 0$. Then $g'(y; t) \equiv 0$ for all $t \geq 0$. Second, let $y = 1$. Then $g'(y; t) \equiv 0$ for all $t \geq 0$. Third, let $y > 1$. Then $g'(y; t) < 0$ for all $t \geq 0$. Fourth, let $y \in (0, 1)$. To prove that $g'(y; t) \leq 1/2$, we determine the global maximum of $g'(y; t)$ with respect to t . Solving $g''(y; t) = 0$ with respect to t , gives that

$$t_{\max} = \frac{1}{2} \log \left(\frac{1}{y} - 1 \right).$$

Noting that t_{\max} exists and that $g'(y; t_{\max}) = 1/2$ for any $y \in (0, 1)$ proves the result. \square

C Proof of Proposition 6.2

Proof. Denote $x = (v_1, u_1)^\top$ and $y = (v_2, u_2)^\top$. We start with Assumption (A1) and have that

$$\begin{aligned}
(N(x) - N(y), x - y) &= \left(\begin{pmatrix} \frac{1}{\epsilon}v_1 - \frac{1}{\epsilon}v_2 - \frac{1}{\epsilon}v_1^3 + \frac{1}{\epsilon}v_2^3 \\ 0 \end{pmatrix}, \begin{pmatrix} v_1 - v_2 \\ u_1 - u_2 \end{pmatrix} \right) \\
&= \frac{1}{\epsilon}(v_1 - v_1^3 - v_2 + v_2^3)(v_1 - v_2) \\
&= \frac{1}{\epsilon}(v_1 - v_2)^2 (1 - (v_1^2 + v_1v_2 + v_2^2)) \\
&\leq \frac{1}{\epsilon}(v_1 - v_2)^2 \leq \frac{1}{\epsilon} \|x - y\|^2.
\end{aligned}$$

Thus, the assumption holds for $c_1 = 1/\epsilon$.

Now, consider Assumption (A2). We have that

$$\begin{aligned}
\|N(x) - N(y)\|^2 &= \left\| \begin{pmatrix} \frac{1}{\epsilon}v_1 - \frac{1}{\epsilon}v_2 + \frac{1}{\epsilon}v_2^3 - \frac{1}{\epsilon}v_1^3 \\ 0 \end{pmatrix} \right\|^2 = \left(\frac{1}{\epsilon}(v_1 - v_2) + \frac{1}{\epsilon}(v_2^3 - v_1^3) \right)^2 \\
&\leq \frac{2}{\epsilon^2}(v_1 - v_2)^2 + \frac{2}{\epsilon^2}(v_2^3 - v_1^3)^2 \\
&= \frac{2}{\epsilon^2}(v_1 - v_2)^2 + \frac{2}{\epsilon^2}(v_2 - v_1)^2 (v_2^2 + v_1v_2 + v_1^2)^2 \\
&\leq \frac{2}{\epsilon^2}(v_1 - v_2)^2 + \frac{16}{\epsilon^2}(v_1 - v_2)^2(v_1^4 + v_2^4),
\end{aligned}$$

where we used again that $v_1v_2 \leq v_1^2 + v_2^2$ and that $(2v_1^2 + 2v_2^2)^2 \leq 8(v_1^4 + v_2^4)$ in the last inequality. Using that $(v_1 - v_2)^2 \leq \|x - y\|^2$ and that $v_1^4 + v_2^4 \leq \|x\|^4 + \|y\|^4$, we finally obtain that

$$\|N(x) - N(y)\|^2 \leq \frac{16}{\epsilon^2} \|x - y\|^2 (1 + \|x\|^4 + \|y\|^4).$$

Thus, the assumption holds for $c_2 = 16/\epsilon^2$ and $\chi = 3$. \square

D Proof of Proposition 6.3

Proof. Part I: We have that

$$M(x; \Delta) = (M_1(v; \Delta), M_2(u; \Delta))^\top = \left(\frac{f_1(v; \Delta) - v}{\Delta}, \frac{f_2(u; \Delta) - u}{\Delta} \right)^\top.$$

Consider the V -component. The fact that for every $\Delta_0 \in (0, 1)$, there exists $c(\Delta_0) > 0$ such that for any $v \in \mathbb{R}$ it holds that

$$|M_1(v; \Delta)| \leq c(\Delta_0)(1 + |v|^4),$$

can be proved in the same way as Lemma 3.4 in [9]. Regarding the U -component, we have that

$$|M_2(u; \Delta)| = \left| \frac{u + \beta\Delta - u}{\Delta} \right| = |\beta| = \beta \leq \beta(1 + |u|^4).$$

Thus,

$$\|M(x; \Delta)\| \leq \left\| \begin{pmatrix} c(\Delta_0)(1 + |v|^4) \\ \beta(1 + |u|^4) \end{pmatrix} \right\| \leq c_3(\Delta_0) \left(1 + \left\| \begin{pmatrix} |v|^4 \\ |u|^4 \end{pmatrix} \right\| \right),$$

which proves that the assumption is satisfied for $q = 2$.

Part II: We have that

$$f(x; \Delta) = (f_1(v; \Delta), f_2(u; \Delta))^\top.$$

Consider the V -component. The fact that, for any $v \in \mathbb{R}$ it holds that

$$f_1^2(v; \Delta) \leq v^2 + c_4 \Delta \quad \forall \Delta \geq 0,$$

where $c_4 = 1/2\epsilon$, can be proved in the same way as Proposition 5.2. Regarding the U -component, by assumption, we have that

$$f_2^2(u; \Delta) = u^2.$$

Thus,

$$\|f(x; \Delta)\|^2 = f_1^2(v; \Delta) + f_2^2(u; \Delta) \leq v^2 + u^2 + c_4 \Delta = \|x\|^2 + c_4 \Delta,$$

which proves the statement. \square

E Proof of Proposition 6.4

Proof. Recall that

$$\|e^{A\Delta}\| = \sqrt{\lambda_{\max}((e^{A\Delta})^\top (e^{A\Delta}))},$$

and define $B := (e^{A\Delta})^\top (e^{A\Delta})$. It suffices to prove that $\lambda_{\max}(B) < 1$ for all $\Delta \in (0, \Delta_0]$.

Since by assumption $\gamma = 1/\epsilon$, κ defined in (43) becomes $\kappa = 4\gamma^2 - 1$. When $\kappa = 0$, this condition is equivalent to $\gamma = 1/2$. In this case, the eigenvalues of B are given by

$$\lambda_1(\Delta) = \frac{1}{2}e^{-\Delta} \left(2 + \Delta^2 - \sqrt{\Delta^2(4 + \Delta^2)} \right) \leq \lambda_2(\Delta) = \frac{1}{2}e^{-\Delta} \left(2 + \Delta^2 + \sqrt{\Delta^2(4 + \Delta^2)} \right).$$

It holds that $\lambda_2'(\Delta) < 0$ for all $\Delta > 0$, where $'$ denotes the derivative with respect to Δ . Thus, $\lambda_2(\Delta)$ is strictly decreasing in Δ . Noting that $\lambda_2(0) = 1$ implies the statement.

When $\kappa > 0$, $\gamma > 1/2$. In this case, the eigenvalues of B are given by

$$\begin{aligned} \lambda_1(\Delta, \gamma) &= \frac{e^{-\Delta}}{\kappa} \left(4\gamma^2 - \cos(\sqrt{\kappa}\Delta) - \sqrt{2[-1 + 8\gamma^2 - \cos(\sqrt{\kappa}\Delta)] \sin^2(\sqrt{\kappa}\Delta/2)} \right), \\ \lambda_2(\Delta, \gamma) &= \frac{e^{-\Delta}}{\kappa} \left(4\gamma^2 - \cos(\sqrt{\kappa}\Delta) + \sqrt{-1 + 8\gamma^2 - 8\gamma^2 \cos(\sqrt{\kappa}\Delta) + \cos^2(\sqrt{\kappa}\Delta)} \right). \end{aligned}$$

Again, we observe that $\lambda_1(\Delta, \gamma) \leq \lambda_2(\Delta, \gamma)$ for all $\Delta > 0$ and $\gamma > 1/2$. Let $\gamma > 1/2$ arbitrary, but fixed. Moreover, define $I_\Delta := \{2\pi l/\sqrt{\kappa}, l \in \mathbb{N}\}$. Since $\cos(2\pi l) = 1$ and $\sin(\pi l) = 0$, we have that

$$\lambda_1(\gamma, \Delta) = \lambda_2(\gamma, \Delta) = e^{-\Delta} < 1, \quad \forall \Delta \in I_\Delta.$$

Let now $\Delta \in (0, \infty) \setminus I_\Delta$. For those values of Δ , the partial derivative of $\lambda_2(\Delta, \gamma)$ with respect to Δ exists. In particular, we have that

$$\frac{\partial}{\partial \Delta} \lambda_2(\Delta, \gamma) < 0, \quad \forall \Delta \in (0, \infty) \setminus I_\Delta.$$

Thus, for a fixed γ , the function $\lambda_2(\Delta, \gamma)$ is strictly decreasing in Δ . Noting that $\lambda_2(0, \gamma) = 1$ for any γ implies the statement. \square